

Exponential Convergence of hp FEM for Spectral Fractional Diffusion in Polygons

Lehel Banjai · Jens M. Melenk ·
Christoph Schwab

the date of receipt and acceptance should be inserted later

Abstract For the spectral fractional diffusion operator of order $2s \in (0, 2)$ in bounded, curvilinear polygonal domains $\Omega \subset \mathbb{R}^2$ we prove exponential convergence of two classes of hp discretizations under the assumption of analytic data (coefficients and source terms, without any boundary compatibility), in the natural fractional Sobolev norm $\mathbb{H}^s(\Omega)$. The first hp discretization is based on writing the solution as a co-normal derivative of a $2 + 1$ -dimensional local, linear elliptic boundary value problem, to which an hp -FE discretization is applied. A diagonalization in the extended variable reduces the numerical approximation of the inverse of the spectral fractional diffusion operator to the numerical approximation of a system of *local, decoupled, second order reaction-diffusion equations in Ω* . Leveraging results on robust exponential convergence

The research of JMM was supported by the Austrian Science Fund (FWF) project F 65. Work performed in part while CS was visiting the Erwin Schrödinger Institute (ESI) in Vienna in June-August 2018 during the ESI thematic period “Numerical Analysis of Complex PDE Models in the Sciences”. Research of CS supported in part by the Swiss National Science Foundation, under Grant SNSF 200021-159940

L. Banjai
Maxwell Institute for Mathematical Sciences
School of Mathematical & Computer Sciences
Heriot-Watt University
Edinburgh EH14 4AS, UK
E-mail: l.banjai@hw.ac.uk

J.M. Melenk
Institut für Analysis und Scientific Computing
Technische Universität Wien
A-1040 Vienna, Austria
E-mail: melenk@tuwien.ac.at

C. Schwab
Seminar for Applied Mathematics
ETH Zürich, ETH Zentrum, HG G57.1
CH8092 Zürich, Switzerland
E-mail: christoph.schwab@sam.math.ethz.ch

of hp -FEM for second order, linear reaction diffusion boundary value problems in Ω , exponential convergence rates for solutions $u \in \mathbb{H}^s(\Omega)$ of $\mathcal{L}^s u = f$ follow. Key ingredient in this hp -FEM are *boundary fitted meshes with geometric mesh refinement towards $\partial\Omega$* .

The second discretization is based on exponentially convergent numerical sinc quadrature approximations of the Balakrishnan integral representation of \mathcal{L}^{-s} combined with hp -FE discretizations of a *decoupled system of local, linear, singularly perturbed reaction-diffusion equations in Ω* . The present analysis for either approach extends to (polygonal subsets \mathcal{M} of) analytic, compact 2-manifolds \mathcal{M} , parametrized by a global, analytic chart χ with polygonal Euclidean parameter domain $\Omega \subset \mathbb{R}^2$. Numerical experiments for model problems in nonconvex polygonal domains and with incompatible data confirm the theoretical results.

Exponentially small bounds on Kolmogoroff n -widths of solutions sets for spectral fractional diffusion in polygons are deduced.

Keywords Fractional diffusion · nonlocal operators · Dunford-Taylor calculus · anisotropic hp -refinement · geometric corner refinement · exponential convergence · n -widths.

Mathematics Subject Classification (2010) 26A33 · 65N12 · 65N30.

1 Introduction

In recent years, the mathematical and numerical analysis of initial-boundary value problems for fractional differential operators has received substantial attention. Their numerical treatment has to overcome several challenges. The first challenge arises from their nonlocal nature as integral operators. A direct Galerkin discretization leads to fully populated system matrices, and compression techniques (see, e.g., [18] and the references there) have to be brought to bear to make the discretization computationally tractable. An alternative to a direct Galerkin discretization of an integral operator, which is possible for the presently considered spectral fractional Laplacian, is to realize the nonlocal operator numerically as a Dirichlet-to-Neumann operator for a local (but degenerate) elliptic problem. While this approach, sometime referred to as “Caffarelli-Silvestre” extension (“CS-extension” for short) [14, 40] increases the spatial dimension by 1, it permits to use the mathematical and numerical tools that were developed for local, integer order differential operators. In the present paper, we study several hp -FE discretizations of the resulting local (but degenerate) elliptic problem, to which we will refer as *Extended hp -FEM*.

One alternative to the extension approach is the representation of fractional powers of elliptic operators as Dunford-Taylor integrals proposed in [9, 10]. Discretizing such an integral leads to a sum of solution operators for *local*, second order elliptic problems, which turn out to be singularly perturbed, but are amenable to established numerical techniques. In the present paper,

we also study this approach under the name *sinc Balakrishnan FEM* (*sinc BK-FEM* for short).

A second challenge arises from the fact that the solutions of problems involving fractional operators are typically not smooth, even for smooth input data (cf. the examples and discussion in [8, Sec. 8.4]). Indeed, for the spectral fractional Laplacian, the behavior near a smooth boundary $\partial\Omega$ is $u \sim u_0 + O(\text{dist}(\cdot, \partial\Omega)^\beta)$ for some more regular u_0 and a $\beta \notin \mathbb{N}$ [15, Thm. 1.3]. Points of non-smoothness of $\partial\Omega$ introduce further singularities into the solution. The numerical resolution of both types of singularities requires suitably designed approximation spaces. For the spectral fractional Laplacian in two-dimensional polygonal domains, we present a class of meshes in Ω with anisotropic, geometric refinement towards $\partial\Omega$ and with isotropic geometric refinement towards the corners of Ω . We show that spaces of piecewise polynomials on such meshes can lead to exponential convergence.

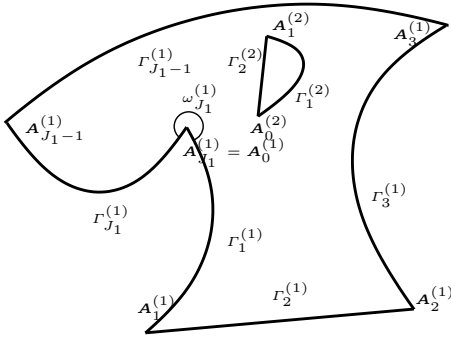


Fig. 1 Example of a curvilinear polygon

1.1 Geometric Preliminaries

As in [7], we consider a bounded Lipschitz domain $\Omega \subset \mathbb{R}^2$ that is a curvilinear polygon as depicted in Fig. 1. The boundary $\partial\Omega$ is assumed to consist of $J \in \mathbb{N}$ closed curves $\Gamma^{(i)}$. Each curve $\Gamma^{(i)}$ in turn is assumed to comprise $J_i \in \mathbb{N}$ many open, disjoint, *analytic arcs* $\Gamma_j^{(i)}$, $j = 1, \dots, J_i$, with $\overline{\Gamma^{(i)}} = \bigcup_{j=1}^{J_i} \overline{\Gamma_j^{(i)}}$, $i = 1, \dots, J$. The arcs $\Gamma_j^{(i)}$ are assumed further to admit *nondegenerate, analytic parametrizations*,

$$\Gamma_j^{(i)} = \left\{ \mathbf{x}_j^{(i)}(\theta) \mid \theta \in (0, 1) \right\}, \quad i = 1, \dots, J, \quad j = 1, \dots, J_i.$$

The coordinate functions $x_j^{(i)}, y_j^{(i)}$ of $\mathbf{x}_j^{(i)}(\theta) = (x_j^{(i)}(\theta), y_j^{(i)}(\theta))$ are assumed to be (real) analytic functions of $\theta \in [0, 1]$ and such that $\min_{\theta \in [0, 1]} |\dot{\mathbf{x}}_j^{(i)}(\theta)|^2 > 0$ for $j = 1, \dots, J_i$, $i = 1, \dots, J$. The end points of the arcs $\Gamma_j^{(i)}$ are denoted as

$\mathbf{A}_{j-1}^{(i)} = \mathbf{x}_j^{(i)}(0)$ and $\mathbf{A}_j^{(i)} = \mathbf{x}_j^{(i)}(1)$. We enumerate these points counterclockwise by indexing cyclically with j modulo J_i , thereby identifying in particular $\mathbf{A}_0^{(i)} := \mathbf{A}_{J_i}^{(i)}$. The interior angle at $\mathbf{A}_j^{(i)}$ is denoted $\omega_j^{(i)} \in (0, 2\pi)$. For notational simplicity, we assume henceforth that $J = 1$, i.e., $\partial\Omega$ consists of a single component of connectedness. We write $\mathbf{A}_j = \mathbf{A}_j^{(1)}$, Γ_j for $\Gamma_j^{(1)}$.

1.2 Spectral Fractional Diffusion

When dealing with fractional operators, care must be exercised in stating the definition of the fractional powers. Here, we consider the so-called *spectral fractional diffusion operators* as investigated in [14]. We refer to the surveys [11, 20, 34] and the references there for a comparison of the different definitions of fractional powers of the Dirichlet Laplacian.

We consider the linear, elliptic, self-adjoint, second order differential operator $w \mapsto \mathcal{L}w = -\operatorname{div}(A\nabla w)$, in a bounded, curvilinear polygon $\Omega \subset \mathbb{R}^2$ as described in Section 1.1. The diffusion coefficient $A \in L^\infty(\Omega, \mathbf{GL}(\mathbb{R}^2))$ is assumed symmetric, uniformly positive definite. The data A and f are assumed analytic in $\bar{\Omega}$. We quantify analyticity of A and f by assuming that there are $C_A, C_f > 0$ such that

$$\forall p \in \mathbb{N}_0 : \quad \|D^p A\|_{L^\infty(\Omega)} \leq C_A^{p+1} p! , \quad \|D^p f\|_{L^\infty(\Omega)} \leq C_f^{p+1} p! . \quad (1.1)$$

Here, the notation $|D^p A|$ signifies $\sum_{|\alpha|=p} |D^\alpha A|$, with the usual multi-index convention D^α denoting mixed weak derivatives of order $\alpha \in \mathbb{N}_0^2$ whose total order $|\alpha| = \alpha_1 + \alpha_2$. Further, we employ standard notation for (fractional) Sobolev spaces $H^t(\Omega)$, consistent with the notation and definitions in [22].

We introduce the “energy” inner product $a_\Omega(\cdot, \cdot)$ on $H_0^1(\Omega)$ associated with the differential operator \mathcal{L} by

$$a_\Omega(w, v) = \int_\Omega (A\nabla w \cdot \nabla v) \, dx' . \quad (1.2)$$

The operator $\mathcal{L} : H_0^1(\Omega) \rightarrow H^{-1}(\Omega)$ induced by this bilinear form is an isomorphism, due to the (assumed) positive definiteness of A . Let $\{\lambda_k, \varphi_k\}_{k \in \mathbb{N}} \subset \mathbb{R}^+ \times H_0^1(\Omega)$ be a sequence of eigenpairs of \mathcal{L} , normalized such that $\{\varphi_k\}_{k \in \mathbb{N}}$ is an orthonormal basis of $L^2(\Omega)$ and an orthogonal basis of $(H_0^1(\Omega), a_\Omega(\cdot, \cdot))$. We introduce, for $\sigma \geq 0$, the domains of fractional powers of \mathcal{L} as

$$\mathbb{H}^\sigma(\Omega) = \left\{ v = \sum_{k=1}^{\infty} v_k \varphi_k : \|v\|_{\mathbb{H}^\sigma(\Omega)}^2 = \sum_{k=1}^{\infty} \lambda_k^\sigma v_k^2 < \infty \right\} . \quad (1.3)$$

We denote by $\mathbb{H}^{-\sigma}(\Omega)$ the dual space of $\mathbb{H}^\sigma(\Omega)$. Denoting by $\langle \cdot, \cdot \rangle$ the $\mathbb{H}^{-\sigma}(\Omega) \times \mathbb{H}^\sigma(\Omega)$ duality pairing that extends the standard $L^2(\Omega)$ inner product, we can identify elements $f \in \mathbb{H}^{-\sigma}(\Omega)$ with sequences $\{f_k\}_k$ (written formally as $\sum_k f_k \varphi_k$) such that $\|f\|_{\mathbb{H}^{-\sigma}(\Omega)}^2 = \sum_k |f_k|^2 \lambda_k^{-\sigma} < \infty$. With this identification, we can extend the definition of the norm in (1.3) to $\sigma < 0$. Furthermore, the

linear operator $\mathcal{L}^s : \mathbb{H}^s(\Omega) \rightarrow \mathbb{H}^{-s}(\Omega) : v \mapsto \sum_{k=1}^{\infty} v_k \lambda_k^s \varphi_k$ is bounded and the Dirichlet problem for the fractional diffusion in Ω may be stated as: given a fractional order $s \in (0, 1]$ and $f \in \mathbb{H}^{-s}(\Omega)$, find $u \in \mathbb{H}^s(\Omega)$ such that

$$\mathcal{L}^s u = f \quad \text{in } \Omega. \quad (1.4)$$

The ellipticity estimate $\langle w, \mathcal{L}^s w \rangle \geq \lambda_1^s \|w\|_{\mathbb{H}^s(\Omega)}^2$ valid for every $w \in \mathbb{H}^s(\Omega)$ implies the unique solvability of (1.4) for every $f \in \mathbb{H}^{-s}(\Omega)$. The hp -FEM approximations of (1.4) developed and analyzed in the present work are not based on explicit or approximated eigenfunctions but instead on the localization of the operator \mathcal{L}^s in terms of extension discussed in Sec. 1.4 and on the Dunford-Taylor integral discussed in Sec. 1.5, the so-called Balakrishnan formula.

Remark 1 (compatibility condition) As discussed in [8, Lemma 1, Rem. 1] the spectral fractional Laplacian has the mapping property $\mathcal{L}^s : \mathbb{H}^{s+\sigma}(\Omega) \rightarrow \mathbb{H}^{-s+\sigma}(\Omega)$, $\sigma \geq 0$. For smooth coefficients A and $\partial\Omega$, the spaces $\mathbb{H}^{s+\sigma}(\Omega)$, $\sigma \geq 0$, are subspaces of the Sobolev spaces $H^{s+\sigma}(\Omega)$. In fact, for $-s+\sigma > 1/2$, the spaces $\mathbb{H}^{-s+\sigma}(\Omega)$ are proper subspaces of $H^{-s+\sigma}(\Omega)$ as they encode some boundary conditions on $\partial\Omega$. E.g., for $f \in \mathbb{H}^{-s+\sigma}(\Omega)$ with $-s+\sigma \geq 1/2$ one has $f|_{\partial\Omega} = 0$. That is, $f \in H^{-s+\sigma}(\Omega)$ must satisfy additionally *compatibility conditions* on $\partial\Omega$ to ensure $u \in H^{s+\sigma}(\Omega)$. ■

1.3 Contributions

We briefly highlight the principal contributions of this work. For the nonlocal, spectral fractional diffusion problem (1.4) in bounded, curvilinear polygonal domains Ω as described in Section 1.1 and with analytic data A and f as in (1.1), and without any boundary compatibility, we develop two hp -FEMs for (1.4) that converge exponentially in terms of the number of degrees of freedom N_{DOF} in Ω . The setting covers in particular also boundary value problems for fractional surface diffusion on analytic surface pieces as in the setting of Section 8.1. Key insight in our error analysis is that either method, based on the extension of (1.4) combined with a diagonalization procedure as in [8, Sec. 6] or on a contour-integral representation of \mathcal{L}^s combined with an exponentially converging sinc quadrature, reduce the numerical solution of (1.4) to the numerical solution of *local, singularly perturbed second order reaction-diffusion problems in Ω* . Drawing on analytic regularity and corresponding hp -FEM in Ω for these reaction-diffusion problems with *robust, exponential convergence* as developed in [7, 27–29], we establish here exponential convergence rate bounds for solutions of (1.4). As we showed in [7, 27], the singular perturbation character of the reaction-diffusion problems in Ω mandates both, *geometric corner mesh refinement* and *anisotropic geometric boundary mesh refinement* to resolve the algebraic corner and boundary singularities that occur in solutions to (1.4).

Before proceeding to the main part of this paper, we briefly recall the localization due to Caffarelli-Silvestre and the contour integral representation of Balakrishnan [6].

1.4 Caffarelli-Silvestre extension

In [14] the (full space) fractional Laplacian \mathcal{L}^s was localized via a singular elliptic PDE depending on one extra variable and thus represented as Dirichlet-to-Neumann problem for an elliptic problem in a half-space. Cabré and Tan [13] and Stinga and Torrea [40] extended this to bounded domains Ω and more general operators, thereby obtaining an extension posed on the semi-infinite cylinder $\mathcal{C} := \Omega \times (0, \infty)$. Their extension is given by the *local boundary value problem*

$$\begin{cases} \mathfrak{L}\mathcal{U} = -\operatorname{div}(y^\alpha \mathfrak{A} \nabla \mathcal{U}) = 0 & \text{in } \mathcal{C} = \Omega \times (0, \infty), \\ \mathcal{U} = 0 & \text{on } \partial_L \mathcal{C}, \\ \partial_{\nu^\alpha} \mathcal{U} = d_s f & \text{on } \Omega \times \{0\}, \end{cases} \quad (1.5)$$

where $\mathfrak{A} = \operatorname{diag}\{A, 1\} \in L^\infty(\mathcal{C}, \operatorname{GL}(\mathbb{R}^{d+1}))$, $\partial_L \mathcal{C} := \partial\Omega \times (0, \infty)$, $d_s := 2^{1-2s}\Gamma(1-s)/\Gamma(s) > 0$ and where $\alpha = 1 - 2s \in (-1, 1)$ [14, 40]. The so-called conormal exterior derivative of \mathcal{U} at $\Omega \times \{0\}$ is

$$\partial_{\nu^\alpha} \mathcal{U} = - \lim_{y \rightarrow 0^+} y^\alpha \mathcal{U}_y. \quad (1.6)$$

The limit in (1.6) is in the distributional sense [13, 14, 40]. Fractional powers of \mathcal{L}^s in (1.4) and the Dirichlet-to-Neumann operator of problem (1.5) are related by [14, 15]

$$d_s \mathcal{L}^s u = \partial_{\nu^\alpha} \mathcal{U} \quad \text{in } \Omega. \quad (1.7)$$

We write $x = (x', y) \in \mathcal{C}$ with $x' \in \Omega$ and $y > 0$. For $D \subset \mathbb{R}^d \times \mathbb{R}^+$, we define $L^2(y^\alpha, D)$ as the Lebesgue space with the measure $y^\alpha dx$ and $H^1(y^\alpha, D)$ as the weighted Sobolev space

$$H^1(y^\alpha, D) := \{w \in L^2(y^\alpha, D) : |\nabla w| \in L^2(y^\alpha, D)\} \quad (1.8)$$

equipped with the norm

$$\|w\|_{H^1(y^\alpha, D)} = \left(\|w\|_{L^2(y^\alpha, D)}^2 + \|\nabla w\|_{L^2(y^\alpha, D)}^2 \right)^{1/2}. \quad (1.9)$$

To investigate (1.5) we include the homogeneous boundary condition on the lateral boundary $\partial_L \mathcal{C}$ by setting

$$\mathring{H}^1(y^\alpha, \mathcal{C}) := \{w \in H^1(y^\alpha, \mathcal{C}) : w = 0 \text{ on } \partial_L \mathcal{C}\}. \quad (1.10)$$

The bilinear form $a_{\mathcal{C}} : \mathring{H}^1(y^\alpha, \mathcal{C}) \times \mathring{H}^1(y^\alpha, \mathcal{C}) \rightarrow \mathbb{R}$ defined by

$$a_{\mathcal{C}}(v, w) = \int_{\mathcal{C}} y^\alpha (\mathfrak{A} \nabla v \cdot \nabla w) dx' dy, \quad (1.11)$$

is continuous and coercive on $\mathring{H}^1(y^\alpha, \mathcal{C})$. The energy norm $\|\cdot\|_{\mathcal{C}}$ on $\mathring{H}^1(y^\alpha, \mathcal{C})$ induced by the inner product $a_{\mathcal{C}}(\cdot, \cdot)$ is given by

$$\|v\|_{\mathcal{C}}^2 := a_{\mathcal{C}}(v, v) \sim \|\nabla v\|_{L^2(y^\alpha, \mathcal{C})}^2. \quad (1.12)$$

For $w \in H^1(y^\alpha, \mathcal{C})$ we denote by $\text{tr}_\Omega w$ its trace on $\Omega \times \{0\}$, which connects the spaces $\mathring{H}^1(y^\alpha, \mathcal{C})$ and $\mathbb{H}^s(\Omega)$ (cf. [31, Prop. 2.5]) via

$$\text{tr}_\Omega \mathring{H}^1(y^\alpha, \mathcal{C}) = \mathbb{H}^s(\Omega), \quad \|\text{tr}_\Omega w\|_{\mathbb{H}^s(\Omega)} \leq C_{\text{tr}_\Omega} \|w\|_{\mathring{H}^1(y^\alpha, \mathcal{C})}. \quad (1.13)$$

With these definitions at hand, the weak formulation of (1.5) is to find

$$\mathcal{U} \in \mathring{H}^1(y^\alpha, \mathcal{C}) : \forall v \in \mathring{H}^1(y^\alpha, \mathcal{C}) : a_{\mathcal{C}}(\mathcal{U}, v) = d_s \langle f, \text{tr}_\Omega v \rangle. \quad (1.14)$$

Remark 2 (regularity of \mathcal{U} for $s = 1/2$) In the special case $s = 1/2$ and $A = \text{Id}$ in (1.4) the operator \mathfrak{L} in the CS extension (1.5) in \mathcal{C} coincides with the Laplacian in \mathcal{C} . Therefore, the solution \mathcal{U} will, in general, exhibit *algebraic singularities* on $\partial\Omega$, even if $\partial\Omega$ is smooth. ■

1.5 Balakrishnan Formula

The second approach we take is via the *spectral integral representation of fractional powers of elliptic operators* going back to [6]. For $0 < s < 1$ and $\mathcal{L} = -\text{div}(A\nabla)$ with homogeneous Dirichlet boundary conditions the bounded linear operator $\mathcal{L}^{-s} : \mathbb{H}^{-s}(\Omega) \rightarrow \mathbb{H}^s(\Omega)$ admits the following representation with $c_B = \pi^{-1} \sin(\pi s)$:

$$\begin{aligned} \mathcal{L}^{-s} &= c_B \int_0^\infty \lambda^{-s} (\lambda I + \mathcal{L})^{-1} d\lambda = c_B \int_{-\infty}^\infty e^{(1-s)y} (e^y I + \mathcal{L})^{-1} dy \\ &= c_B \int_{-\infty}^\infty e^{-sy} (I + e^{-y} \mathcal{L})^{-1} dy. \end{aligned} \quad (1.15)$$

The representations (1.15) were used in [9, 10] in conjunction with an exponentially convergent, so-called sinc quadrature approximation of (1.15) (see, e.g., [39] for details) and an h -version Finite Element projection in Ω to obtain numerical approximations of the fractional diffusion equation (1.4) in Ω . Here, we generalize the results in [9, 10] to the hp -FEM, establishing exponential convergence rates in polygonal domains Ω for the resulting sinc BK-FEM for data A and f that are analytic in $\bar{\Omega}$ (cf. (1.1)) without boundary compatibility of f .

1.6 Outline

The outline of the remainder of the paper is as follows. The following Section 2 describes the hp -FE spaces and Galerkin methods for (1.5) based on tensor products of discretizations in the x and the y variable.

Section 3 develops the diagonalization of the hp -FE semi-discretization in the extended variable. In particular, in Section 3.1 we prove exponential convergence of an hp -FE *semidiscretization* in $(0, \infty)$. The diagonalization reduces the semidiscrete approximation of the CS-extended, localized problem to a collection of decoupled, linear second order reaction-diffusion problems in Ω .

Section 4 presents the exponential convergence results from [7] of hp -FE discretizations of linear, second order singularly perturbed reaction-diffusion equations in Ω and establishes robust (with respect to the perturbation parameter ε) exponential convergence results for these.

Section 5 completes the proof of exponential convergence for the Extended hp -FEM by applying the hp -FEM from Section 4 in Ω for the reaction-diffusion problems obtained from the diagonalization process in Section 3. Section 5 presents in fact two distinct hp -FE discretizations: a pure Galerkin method (**Case B**) and a method based on discretizing after diagonalization each decoupled problem separately (**Case A**). The latter approach features slightly better complexity estimates.

Section 6 is devoted to the analysis of the sinc BK-FEM. There once more the numerical approximation of the fractional Laplacian is reduced to the numerical solution of a sequence of *local* linear, second order reaction-diffusion problems in Ω . Applying exponential convergence bounds for sinc approximation and for hp -FEM for reaction-diffusion problems in Ω in Section 4 from [7], once again exponential convergence for the resulting sinc BK-FEM for the spectral version of the fractional diffusion operator is established. As in Section 5, we separately discuss the possibilities of approximating the solutions of the decoupled problems from the same space (**Case B**) or from different spaces (**Case A**). Section 7 has numerical experiments verifying the theoretical convergence results. Section 8 has a summary and outlines several generalizations and directions for further research. In particular, we address in Section 8.1 the extension to fractional diffusion on manifolds. In Section 8.2, we discuss several exponential bounds on Kolmogoroff n -widths of solution sets for spectral diffusion in polygons that follow from our results.

1.7 Notation

Constants C , γ , b may be different in each occurrence, but are independent of critical parameters. We denote by $\hat{S} := (0, 1)^2$ the reference square and by $\hat{T} := \{(\xi_1, \xi_2) \mid 0 < \xi_1 < 1, 0 < \xi_2 < \xi_1\}$ the reference triangle. Sets of the form $\{x = y\}$, $\{x = 0\}$, $\{x = y\}$ etc. refer to edges and diagonals of \hat{S} and analogously $\{y \leq x\} = \{(x, y) \in \hat{S} \mid y \leq x\}$. \mathbb{P}_q denotes the space of

polynomials of total degree q and \mathbb{Q}_q the tensor product space of polynomial of degree q in each variable separately.

2 hp -FEM Discretization

In this section, we introduce some hp -FEM space in both the x and the y -variable on which the Extended hp -FEM will be based. In particular, we introduce the geometric meshes $\mathcal{G}_{geo,\sigma}^M$ that are used for the discretization in the y -variable.

2.1 Notation and FE spaces

2.1.1 Meshes and FE spaces on $(0, \mathcal{Y})$

Given a truncation parameter \mathcal{Y} and a mesh $\mathcal{G}^M = \{I_m\}_{m=1}^M$ in $[0, \mathcal{Y}]$ consisting of M intervals $I_m = [y_{m-1}, y_m]$, with $0 = y_0 < y_1 < \dots < y_M = \mathcal{Y}$, we associate to \mathcal{G}^M a *polynomial degree distribution* $\mathbf{r} = (r_1, r_2, \dots, r_M) \in \mathbb{N}^M$. We introduce the hp -FE space

$$S^{\mathbf{r}}((0, \mathcal{Y}), \mathcal{G}^M) = \{v_M \in H^1(\mathbb{R}) : \text{supp } v \subset [0, \mathcal{Y}], \\ v_M|_{I_m} \in \mathbb{P}_{r_m}(I_m), I_m \in \mathcal{G}^M, m = 1, \dots, M\},$$

where \mathbb{P}_r denotes the space of polynomials of degree r . We will primarily work with the following piecewise polynomial space $S_{\{\mathcal{Y}\}}^{\mathbf{r}}((0, \mathcal{Y}), \mathcal{G}^M) \subset H^1(0, \infty)$ of functions that vanish on $[\mathcal{Y}, \infty)$:

$$S_{\{\mathcal{Y}\}}^{\mathbf{r}}((0, \mathcal{Y}), \mathcal{G}^M) = \{v \in S^{\mathbf{r}}((0, \mathcal{Y}), \mathcal{G}^M) : v(\mathcal{Y}) = 0\}. \quad (2.1)$$

For constant polynomial degree $r_i = r \geq 1, i = 1, \dots, M$, we set $S_{\{\mathcal{Y}\}}^r((0, \mathcal{Y}), \mathcal{G}^M)$. Henceforth, we abbreviate

$$\mathcal{M} := \dim S_{\{\mathcal{Y}\}}^{\mathbf{r}}((0, \mathcal{Y}), \mathcal{G}^M) \sim M^2 \text{ as } M \rightarrow \infty. \quad (2.2)$$

Of particular interest will be *geometric meshes* $\mathcal{G}_{geo,\sigma}^M$ on $[0, \mathcal{Y}]$, with M elements and grading factor $\sigma \in (0, 1)$: $\{I_i | i = 1, \dots, M\}$ with elements $I_1 = [0, \mathcal{Y}\sigma^{M-1}]$ and $I_i = [\mathcal{Y}\sigma^{M-i+1}, \mathcal{Y}\sigma^{M-i}]$ for $i = 2, \dots, M$. On geometric meshes $\mathcal{G}_{geo,\sigma}^M$ on $[0, \mathcal{Y}]$, we consider a *linear polynomial degree vector* $\mathbf{r} = \{r_i\}_{i=1}^M$ with *slope* $\mathfrak{s} > 0$ which is defined by

$$r_i := 1 + \lceil \mathfrak{s}(i-1) \rceil, \quad i = 1, 2, \dots, M. \quad (2.3)$$

For geometric meshes and linear degree vectors we set

$$\mathcal{M}_{geo} := \dim S_{\{\mathcal{Y}\}}^{\mathbf{r}}((0, \mathcal{Y}), \mathcal{G}^M) \sim M^2 \text{ as } M \rightarrow \infty \quad (2.4)$$

with constants implied in \sim depending on $\mathfrak{s} > 0$.

2.1.2 *hp-FEM in Ω*

In the polygon Ω , we consider Lagrangian FEM of uniform¹ polynomial degree $q \geq 1$ based on regular triangulations of Ω denoted by \mathcal{T} . We admit both triangular and quadrilateral elements $K \in \mathcal{T}$, but *do not* assume shape regularity. In fact, as we shall explain in Section 4 ahead, *anisotropic mesh refinement towards $\partial\Omega$* will be required to resolve singularities at the singular support $\partial\Omega$ that are generically present in solutions of fractional PDEs (cf. Remark 2). We introduce, for a regular (in the sense of [27, Def. 2.4.1]) triangulation \mathcal{T} of Ω comprising curvilinear triangular or quadrilateral elements $K \in \mathcal{T}$ with associated analytic element maps $F_K : \hat{K} \rightarrow K$ (where $\hat{K} \in \{\hat{T}, \hat{S}\}$ is either the reference triangle or square depending on whether K is a curvilinear triangle or quadrilateral) the FE space

$$S_0^q(\Omega, \mathcal{T}) = \left\{ v_h \in C(\bar{\Omega}) : v_h|_K \circ F_K \in V_q(\hat{K}) \quad \forall K \in \mathcal{T}, \quad v_h|_{\partial\Omega} = 0 \right\}. \quad (2.5)$$

Here, for $q \geq 1$, the local polynomial space $V_q(\hat{K}) = \mathbb{P}_q$ if $\hat{K} = \hat{T}$ and $V_q(\hat{K}) = \mathbb{Q}_q$ if $\hat{K} = \hat{S}$.

2.1.3 *Tensor product hp-FE approximation*

One *hp*-FE approximation of the extended problem (1.5) will be based on the finite-dimensional *tensor product spaces* of the form

$$\mathbb{V}_{h,M}^{q,r}(\mathcal{T}, \mathcal{G}^M) := S_0^q(\Omega, \mathcal{T}) \otimes S_{\{\mathcal{Y}\}}^r((0, \mathcal{Y}), \mathcal{G}^M) \subset \mathring{H}^1(y^\alpha, \mathcal{C}), \quad (2.6)$$

where \mathcal{T} is a regular triangulation of Ω . To analyze this method, we consider semidiscretizations based on the following (infinite-dimensional, closed) Hilbertian tensor product space:

$$\mathbb{V}_M^r(\mathcal{C}_{\mathcal{Y}}) := H_0^1(\Omega) \otimes S_{\{\mathcal{Y}\}}^r((0, \mathcal{Y}), \mathcal{G}^M) \subset \mathring{H}^1(y^\alpha, \mathcal{C}). \quad (2.7)$$

Here, the argument $\mathcal{C}_{\mathcal{Y}}$ indicates that spaces of functions supported in $\bar{\Omega} \times [0, \mathcal{Y}]$ are considered. Galerkin projections onto the spaces $\mathbb{V}_{h,M}^{q,r}(\mathcal{T}^q, \mathcal{G}^M)$ and $\mathbb{V}_M^r(\mathcal{C}_{\mathcal{Y}})$ with respect to the inner product $a_{\mathcal{C}}(\cdot, \cdot)$ are denoted by $G_{h,M}^{q,r}$ and G_M^r , respectively. For the CS-extension \mathcal{U} , i.e., the solution of (1.14), the Galerkin projections $G_{h,M}^{q,r}\mathcal{U}$ and $G_M^r\mathcal{U}$ are characterized by

$$a_{\mathcal{C}}(G_{h,M}^{q,r}\mathcal{U}, v) = d_s \langle f, \text{tr}_{\Omega} v \rangle \quad \forall v \in \mathbb{V}_{h,M}^{q,r}(\mathcal{T}, \mathcal{G}^M), \quad (2.8)$$

$$a_{\mathcal{C}}(G_M^r\mathcal{U}, v) = d_s \langle f, \text{tr}_{\Omega} v \rangle \quad \forall v \in \mathbb{V}_M^r(\mathcal{T}, \mathcal{G}^M). \quad (2.9)$$

¹ We adopt uniform polynomial degree $q \geq 1$ here to ease notation and presentation. All approximation results admit lower degrees in certain parts of the triangulations. This will affect, however, only constants in the error bounds, and will not affect convergence rates in the ensuing exponential convergence estimates.

3 Approximation based on semidiscretization in y

A key step in the hp -FE discretization in $(0, \mathcal{Y})$ is, as in [8], the *diagonalization* of the semidiscretized, truncated extension problem with solution $G_M^{\mathbf{r}} \mathcal{U}$ given by (2.9).

3.1 Exponential Convergence of hp -FEM in $(0, \infty)$

As in [8, 23], we exploit the analytic regularity of the extended solution \mathcal{U} with respect to the extended variable y . It results in *exponential convergence* of the hp -semidiscretization error $\mathcal{U} - G_M^{\mathbf{r}} \mathcal{U}$ in $(0, \mathcal{Y})$, if geometric meshes $\mathcal{G}_{geo, \sigma}^M$ and a truncation parameter $\mathcal{Y} \sim M$ are used.

Lemma 1 (exponential convergence, [8, Lemma 6.2]) *Fix $c_1 < c_2$. Let $f \in \mathbb{H}^{-s+\nu}(\Omega)$ for some $\nu \in (0, s)$. Assume that \mathcal{Y} satisfies $c_1 M \leq \mathcal{Y} \leq c_2 M$, and consider the geometric mesh $\mathcal{G}_{geo, \sigma}^M$ on $(0, \mathcal{Y})$ and the linear degree vector \mathbf{r} with slope $\mathfrak{s} > 0$. Let \mathcal{U} be given by (1.14) and $G_M^{\mathbf{r}} \mathcal{U}$ be the Galerkin projection onto $\mathbb{V}_M^{\mathbf{r}}(\mathcal{T}, \mathcal{G}^M)$ given by (2.9). Then there exist $C, b > 0$ (depending solely on $s, \mathcal{L}, c_1, c_2, \sigma, \nu, \mathfrak{s}$) such that*

$$\|\nabla(\mathcal{U} - G_M^{\mathbf{r}} \mathcal{U})\|_{L^2(y^\alpha, \mathcal{C})} \leq C e^{-bM} \|f\|_{\mathbb{H}^{-s+\nu}(\Omega)}. \quad (3.1)$$

Furthermore, (3.1) also holds for constant polynomial degree $\mathbf{r} = (r, \dots, r)$ if $c_3 M \leq r \leq c_4 M$ for some fixed $c_3, c_4 > 0$. The constant $b > 0$ then depends additionally on c_3, c_4 .

Proof The statement is a slight generalization of [8, Lemma 13]. In [8, Lemma 13], it is stated that the slope \mathfrak{s} has to satisfy $\mathfrak{s} \geq \mathfrak{s}_{min}$ for some suitable $\mathfrak{s}_{min} > 0$. Inspection of the proof shows that this condition can be removed. Specifically, using [2, Thm. 8, Eqn. (78), Rem. 16] (or, referring alternatively to the extended preprint [2, Thm. 3.13, Eqn. (3.21), Rem. 3.14]) the result holds for any $\mathfrak{s} > 0$, with constant $b = O(\mathfrak{s})$ as $\mathfrak{s} \downarrow 0$. The statement about the constant polynomial degree follows from the case of the linear degree vector since a) $G_M^{\mathbf{r}} \mathcal{U}$ is the Galerkin projection of \mathcal{U} , b) the minimization property of Galerkin projections, and c) the fact that the space $S_{\{\mathcal{Y}\}}^{\mathbf{r}}((0, \mathcal{Y}), \mathcal{G}_{geo, \sigma}^M)$ is a subspace of $S_{\{\mathcal{Y}\}}^{\mathbf{r}}((0, \mathcal{Y}), \mathcal{G}_{geo, \sigma}^M)$ provided \mathbf{r} is a linear degree vector with suitably chosen slope.

The error bound (3.1) shows that up to an exponentially small (with respect to \mathcal{Y}) error introduced by truncation of $(0, \infty)$ at \mathcal{Y} , the solution \mathcal{U} can be approximated by the solution of a local problem on the finite cylinder $\mathcal{C}_{\mathcal{Y}}$.

3.2 Diagonalization

Diagonalization, as introduced in [8], refers to the observation that the solution $G_M^{\mathbf{r}} \mathcal{U}$ of the semidiscrete problem (2.9) can be expressed in terms of \mathcal{M} solutions $U_i \in H_0^1(\Omega)$, of \mathcal{M} *decoupled, linear local 2nd order reaction-diffusion*

problems in Ω . As the eigenvalues μ_i in the corresponding eigenvalue problem (3.2) ahead govern the length scales in the *local* reaction-diffusion problems in Ω (3.5) (which, in turn, will be crucial in the mesh-design for the *hp*-FEM in Ω), it is of interest to know their asymptotic behavior. We investigate this in Lemma 2 below.

Diagonalization is based on the explicit representation for the semidiscrete solution \mathcal{U}_M obtained from the following generalized eigenvalue problem, introduced in [8, Sec. 6], and proposed earlier in [21], which reads: find $(v, \mu) \in S_{\{\mathcal{Y}\}}^{\mathbf{r}}((0, \mathcal{Y}), \mathcal{G}^M) \setminus \{0\} \times \mathbb{R}$ such that

$$\forall w \in S_{\{\mathcal{Y}\}}^{\mathbf{r}}((0, \mathcal{Y}), \mathcal{G}^M) : \quad \mu \int_0^{\mathcal{Y}} y^\alpha v'(y) w'(y) \, dy = \int_0^{\mathcal{Y}} y^\alpha v(y) w(y) \, dy. \quad (3.2)$$

All eigenvalues $(\mu_i)_{i=1}^{\mathcal{M}}$ of (3.2) are positive and $S_{\{\mathcal{Y}\}}^{\mathbf{r}}((0, \mathcal{Y}), \mathcal{G}^M)$ has an orthonormal eigenbasis $(v_i)_{i=1}^{\mathcal{M}}$ satisfying

$$\int_0^{\mathcal{Y}} y^\alpha v_i'(y) v_j'(y) \, dy = \delta_{i,j}, \quad \int_0^{\mathcal{Y}} y^\alpha v_i(y) v_j(y) \, dy = \mu_i \delta_{i,j}. \quad (3.3)$$

We may expand the semidiscrete approximation $G_M^{\mathbf{r}} \mathcal{U}$ as

$$G_M^{\mathbf{r}} \mathcal{U}(x', y) =: \sum_{i=1}^{\mathcal{M}} U_i(x') v_i(y). \quad (3.4)$$

The coefficient functions $U_i \in H_0^1(\Omega)$ satisfy a system of \mathcal{M} *decoupled* linear reaction-diffusion equations in Ω : for $i = 1, \dots, \mathcal{M}$, find $U_i \in H_0^1(\Omega)$ such that

$$\forall V \in H_0^1(\Omega) : \quad a_{\mu_i, \Omega}(U_i, V) = d_s v_i(0) \langle f, V \rangle. \quad (3.5)$$

Here v_i denotes the i -th eigenfunction of the eigenvalue problem (3.2), (3.3) and

$$a_{\mu_i, \Omega}(U, V) := \mu_i a_\Omega(U, V) + \int_\Omega UV \, dx', \quad (3.6)$$

with a_Ω as introduced in (1.2). Due to the biorthogonality (3.3) of the discrete eigenfunctions $v_i \in S_{\{\mathcal{Y}\}}^{\mathbf{r}}((0, \mathcal{Y}), \mathcal{G}^M)$, any $Z(x', y) = \sum_{i=1}^{\mathcal{M}} V_i(x') v_i(y)$ with arbitrary $V_i \in H_0^1(\Omega)$ satisfies the energy (“Pythagoras”) identities

$$a_{\mathcal{C}}(Z, Z) = a_{\mathcal{C}_{\mathcal{Y}}}(Z, Z) = \sum_{i=1}^{\mathcal{M}} \|V_i\|_{\mu_i, \Omega}^2, \quad \|V_i\|_{\mu_i, \Omega}^2 := a_{\mu_i, \Omega}(V_i, V_i). \quad (3.7)$$

The following bounds on the μ_i were shown in [8, Lemma 14] for the special case of geometric meshes $\mathcal{G}_{geo, \sigma}^M$ and linear degree vectors:

Lemma 2 (properties of the eigenpairs, [8, Lemma 14]) *Let $\{\mathcal{G}_{geo, \sigma}^M\}_{M \geq 1}$ be a sequence of geometric meshes on $(0, \mathcal{Y})$ and \mathbf{r} a linear polynomial degree vector with slope $\mathfrak{s} > 0$.*

Assume that the truncation parameter \mathcal{Y} is chosen so that $c_1 M \leq \mathcal{Y} \leq c_2 M$ for some constants $0 < c_1, c_2 < \infty$ that are independent of M .

Then, there exists $C > 1$ (depending on c_1, c_2 and on $\sigma \in (0, 1)$) such that there holds for every $M \in \mathbb{N}$ for the eigenpairs $(\mu_i, v_i)_{i=1}^{\mathcal{M}_{geo}}$ given by (3.2), (3.3)

$$\|v_i\|_{L^\infty(0, \mathcal{Y})} \leq CM^{(1-\alpha)/2}, \quad C^{-1}(\mathfrak{s}^{-2}M^{-2}\sigma^M)^2 \leq \mu_i \leq CM^2. \quad (3.8)$$

3.3 Fully discrete approximation

The full discretization is obtained by approximating the functions U_i of (3.5) from finite-dimensional spaces. Let $\mathcal{T}_i, i = 1, \dots, \mathcal{M}$, be regular triangulations in Ω and $q \in \mathbb{N}$. Let $\Pi_i^q : H_0^1(\Omega) \rightarrow S_0^q(\Omega, \mathcal{T}_i)$ denote the Ritz projectors for the bilinear forms $a_{\mu_i, \Omega}$, which are characterized by

$$a_{\mu_i, \Omega}(u - \Pi_i^q u, v) = 0 \quad \forall v \in S_0^q(\Omega, \mathcal{T}_i). \quad (3.9)$$

In terms of the projections Π_i^q we can define the fully discrete approximation

$$\mathcal{U}_{h, M}(x, y) := \sum_{i=1}^{\mathcal{M}} v_i(y) \Pi_i^q U_i(x). \quad (3.10)$$

By combining (3.5) and (3.9), the functions $\Pi_i^q U_i \in S_0^q(\Omega, \mathcal{T}_i)$ are explicitly and computably given as the solutions of

$$\forall V \in S_0^q(\Omega, \mathcal{T}_i) : a_{\mu_i, \Omega}(\Pi_i^q U_i, V) = d_s v_i(0) \langle f, V \rangle. \quad (3.11)$$

In view of (3.7), we have the following representation of the difference between the semidiscrete approximation $G_M^{\mathbf{r}} \mathcal{U}$ and the fully discrete approximation $\mathcal{U}_{h, M}$:

Lemma 3 *Let $\mathcal{U}_{h, M}$ be given by (3.10). Then:*

$$a_{\mathcal{C}}(G_M^{\mathbf{r}} \mathcal{U} - \mathcal{U}_{h, M}, G_M^{\mathbf{r}} \mathcal{U} - \mathcal{U}_{h, M}) = \sum_{i=1}^{\mathcal{M}} \|U_i - \Pi_i^q U_i\|_{\mu_i, \Omega}^2. \quad (3.12)$$

Concerning the meshes \mathcal{T}_i , we distinguish two cases in this work:

Case A: The meshes $\mathcal{T}_i, i = 1, \dots, \mathcal{M}$, possibly differ from each other.

Case B: The meshes $\mathcal{T}_i, i = 1, \dots, \mathcal{M}$, coincide. That is, all coefficient functions U_i in the semidiscrete solution (3.4) are approximated from one common hp -FE space $S_0^q(\Omega, \mathcal{T})$.

In **Case B** the approximation $\mathcal{U}_{h, M}$ actually coincides with the Galerkin projection $G_{h, M}^{q, \mathbf{r}} \mathcal{U} \in \mathbb{V}_{h, M}^{q, \mathbf{r}}(\mathcal{T}, \mathcal{G}^M) = S_0^q(\Omega, \mathcal{T}) \otimes S_{\{\mathcal{Y}\}}^{\mathbf{r}}((0, \mathcal{Y}), \mathcal{G}^M)$:

Lemma 4 (error representation, [8, Lemma 12]) *Let $(\mu_i, v_i)_{i=1}^{\mathcal{M}}$ be the eigenpairs given by (3.2), (3.3). For $i = 1, \dots, \mathcal{M}$, let $U_i \in H_0^1(\Omega)$ be the solutions to (3.5). Consider **Case B** and let $\Pi_i^q : H_0^1(\Omega) \rightarrow S_0^q(\Omega, \mathcal{T})$ be the Galerkin projections given as in (3.9), with one common, regular triangulation \mathcal{T} of Ω for $i = 1, \dots, \mathcal{M}$. Let $G_M^{\mathbf{r}} \mathcal{U}$ denote the solution to the semidiscrete problem (2.9). Then the tensor product Galerkin approximation $G_{h,M}^{q,\mathbf{r}} \mathcal{U} \in \mathbb{V}_{h,M}^{q,\mathbf{r}}(\mathcal{T}, \mathcal{G}^M) = S_0^q(\Omega, \mathcal{T}) \otimes S_{\{\mathcal{Y}\}}^{\mathbf{r}}((0, \mathcal{Y}), \mathcal{G}^M)$ satisfies*

$$\mathcal{U}_{h,M}(x', y) = \sum_{i=1}^{\mathcal{M}} v_i(y) \Pi_i^q U_i(x'), \quad (3.13)$$

$$a_C(G_M^{\mathbf{r}} \mathcal{U} - G_{h,M}^{q,\mathbf{r}} \mathcal{U}, G_M^{\mathbf{r}} \mathcal{U} - G_{h,M}^{q,\mathbf{r}} \mathcal{U}) = \sum_{i=1}^{\mathcal{M}} \|U_i - \Pi_i^q U_i\|_{\mu_i, \Omega}^2. \quad (3.14)$$

Lemma 4 shows that in **Case B**, the Galerkin projection of \mathcal{U} into the tensor product space $\mathbb{V}_{h,M}^{q,\mathbf{r}}(\mathcal{T}, \mathcal{G}^M)$ coincides with the approximation $\mathcal{U}_{h,M}$ defined in (3.10) in terms of the decoupling procedure. Hence, the decoupling procedure is not essential for numerical purposes in **Case B**, although it has algorithmic advantages. In contrast, **Case A** relies on the decoupling in an essential way. In both cases, the exponential convergence result below will make use of the error estimates of Lemmas 3, 4 obtained by the diagonalization process.

It is advisable to choose the spaces \mathcal{T}_i in case **Case A** such that the functions U_i can be approximated well from $S_0^q(\Omega, \mathcal{T}_i)$ in the norm $\|\cdot\|_{\mu_i, \Omega}$. Correspondingly in **Case B**, the common space \mathcal{T} should be chosen such that each U_i can be approximated well from $S_0^q(\Omega, \mathcal{T})$. The bounds (3.8) indicate that, for large M , most of the reaction-diffusion problems (3.5) are singularly perturbed. Hence we design in the following Section 4 *hp*-FE approximation spaces in Ω which afford exponential convergence rates that are *robust* with respect to the singular perturbation parameter.

4 *hp*-FE Approximation of singular perturbation problems

In the exponential convergence rate analysis of tensorized *hp*-FEM for the CS extension (Extended *hp*-FEM) as well as for the ensuing (see Section 6 ahead) sinc BK-FEM approximation, a crucial role is played by *robust exponential convergence rate bounds for *hp*-FEM for singularly perturbed, reaction-diffusion problems* in curvilinear polygonal domains Ω . Specifically, we consider the *hp*-FE approximation of the local reaction-diffusion problem in Ω ,

$$-\varepsilon^2 \operatorname{div}(A(x') \nabla u^\varepsilon) + c(x') u^\varepsilon = f \quad \text{in } \Omega, \quad u^\varepsilon = 0 \quad \text{on } \partial\Omega, \quad (4.1)$$

where we assume $\operatorname{ess\,inf}_{x' \in \Omega} c(x') \geq c_0 > 0$ and

$$\begin{aligned} &A, c, \text{ and } f \text{ are analytic on } \overline{\Omega} \text{ and} \\ &A \text{ is symmetric, uniformly positive definite.} \end{aligned} \quad (4.2)$$

We note again that (4.1) does not imply any kind of boundary compatibility of f at $\partial\Omega$ (cf. Remark 1). We assume Ω to be scaled so that $\text{diam}(\Omega) = O(1)$. Then, for small $\varepsilon > 0$, the boundary value problem (4.1) is a so-called “elliptic-elliptic” singular perturbation problem. Under the assumptions (4.2), for every $\varepsilon > 0$ problem (4.1) admits a unique solution $u^\varepsilon \in H_0^1(\Omega)$. In general, u^ε exhibits, for small $\varepsilon > 0$, *boundary layers near $\partial\Omega$* whose robust numerical resolution (i.e., with error bounds whose constants are independent of ε) requires *anisotropically refined meshes aligned with $\partial\Omega$* (see [17, 28, 33] and the references there). In addition, the corners of Ω induce point singularities in the (analytic in Ω) solution u^ε . In the context of *hp*-FEM under consideration here, their efficient numerical approximation mandates *geometric mesh refinement near the corners*.

In the present section, we consider the *hp*-FEM approximation of u^ε that features exponential convergence for two different types of meshes: a) *geometric boundary layer meshes* in Section 4.2 and b) *admissible boundary layer meshes* in Section 4.3. In both cases the error estimates are of the form $O(e^{-bq} + e^{-b'L})$, with the constant hidden in $O(\cdot)$ independent of ε , L , and q and where q is the polynomial degree employed and L measures the number of layers of geometric refinement towards the vertices or edges of Ω . The difference in these two types of meshes is that “admissible boundary layer meshes” are strongly ε -dependent with geometric refinement towards the vertices and only a *single* layer of thin elements of width $O(q\varepsilon)$ near $\partial\Omega$ to resolve the boundary layer. The number of elements is then $O(L)$ leading to a number of degrees of freedom $N = O(Lq^2)$. In contrast, geometric boundary layer meshes are based on geometric, anisotropic refinement towards the edges and corners of Ω . As we show in [7], *hp*-FEM on such meshes afford exponential convergence for boundary layers with multiple scales. The total number of elements in geometric boundary layer meshes with L layers is $O(L^2)$. Combined with local FE spaces of polynomial degree q , this results in a number of degrees of freedom $N = O(L^2q^2)$. Whereas *admissible boundary layer meshes* are designed to approximate boundary layers of a single, given length scale ε , geometric boundary layer meshes afford concurrent, robust and exponentially convergent approximations of boundary layers with multiple length scales in Ω . These arise, e.g., upon semidiscretization in the extended variable as is evident from (3.5).

4.1 Macro triangulation. Geometric boundary layer mesh

We do not consider the most general meshes with anisotropic refinement, but confine the *hp*-FE approximation theory to meshes generated as push-forwards of a small number of so-called *mesh patches*. This concept was used in the error analysis of *hp*-FEM for singular perturbations in [27, Sec. 3.3.3] and in [17]. Specifically, we assume given a *fixed macro-triangulation* $\mathcal{T}^\mathcal{M} = \{K^\mathcal{M} \mid K^\mathcal{M} \in \mathcal{T}^\mathcal{M}\}$ of Ω consisting of curvilinear quadrilaterals $K^\mathcal{M}$ with analytic *patch maps* (to be distinguished from the actual element maps) $F_{K^\mathcal{M}} : \hat{S} = (0, 1)^2 \rightarrow K^\mathcal{M}$ that satisfy the usual compatibility conditions. I.e., $\mathcal{T}^\mathcal{M}$ does not have

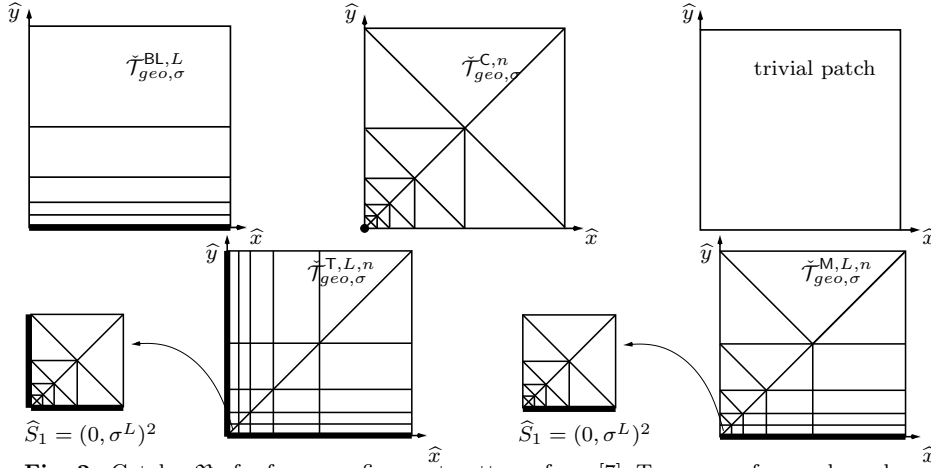


Fig. 2 Catalog \mathfrak{P} of reference refinement patterns from [7]. Top row: reference boundary layer patch $\tilde{\mathcal{T}}_{geo,\sigma}^{BL,L}$ with L layers of geometric refinement towards $\{\hat{y} = 0\}$; reference corner patch $\tilde{\mathcal{T}}_{geo,\sigma}^{C,n}$ with n layers of geometric refinement towards $(0,0)$; trivial patch. Bottom row: reference tensor patch $\tilde{\mathcal{T}}_{geo,\sigma}^{T,L,n}$ with n layers of refinement towards $(0,0)$ and L layers of refinement towards $\{\hat{x} = 0\}$ and $\{\hat{y} = 0\}$; reference mixed patch $\tilde{\mathcal{T}}_{geo,\sigma}^{M,L,n}$ with L layers of refinement towards $\{\hat{y} = 0\}$ and n layers of refinement towards $(0,0)$. Geometric entities shown in boldface indicate parts of $\partial\hat{S}$ that are mapped to $\partial\Omega$. These patch meshes are transported into the curvilinear polygon Ω shown in Fig. 1 via analytic patch maps $F_{K\mathcal{M}}$.

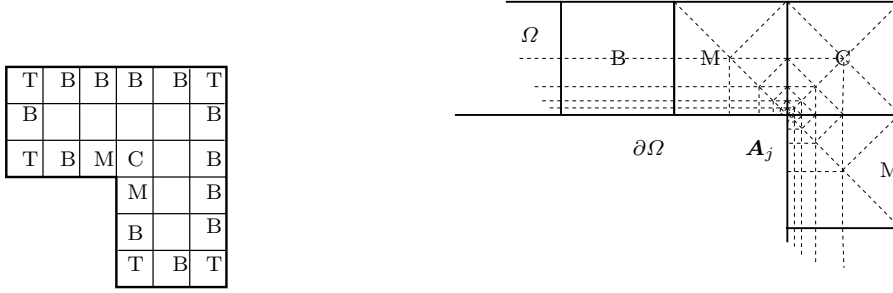


Fig. 3 Patch arrangement in Ω [7]. Left panel: example of L-shaped domain decomposed into 27 patches (T , B , M , C indicate Tensor, Boundary layer, Mixed, Corner patches, empty squares stand for trivial patches). Right panel: Zoom-in near the reentrant corner A_j . Solid lines indicate patch boundaries, dashed lines mesh lines.

hanging nodes and, for any two distinct elements $K_1^{\mathcal{M}}, K_2^{\mathcal{M}} \in \mathcal{T}^{\mathcal{M}}$ that share an edge e , their respective element maps induce compatible parametrizations of e (cf., e.g., [27, Def. 2.4.1] for the precise conditions). Each element of the fixed macro-triangulation $\mathcal{T}^{\mathcal{M}}$ is further subdivided according to one of the refinement patterns in Definition 1 (see also [27, Sec. 3.3.3] or [17]). The actual triangulation is then obtained by transplanting refinement patterns on the square reference patch into the physical domain Ω by means of the element maps $F_{K\mathcal{M}}$ of the macro-triangulation. That is, for any element $K \in \mathcal{T}$, the element map F_K is the concatenation of an affine map—which realizes the

mapping from the reference square or triangle to the elements in the patch refinement pattern and will be denoted by A_K — and the patch map (which will be denoted by $F_{K\mathcal{M}}$), i.e., $F_K = F_{K\mathcal{M}} \circ A_K : \hat{K} \rightarrow K$.

The following refinement patterns were introduced in [7, Def. 2.1, 2.3]. They are based on geometric refinement towards a vertex and/or an edge; the integer L controls the number of layers of refinement towards an edge whereas $n \in \mathbb{N}$ measures the refinement towards a vertex.

Definition 1 (Catalog \mathfrak{P} of refinement patterns, [7, Def. 2.1]) Given $\sigma \in (0, 1)$, $L, n \in \mathbb{N}_0$ with $n \geq L$ the catalog \mathfrak{P} consists of the following patterns:

1. The *trivial patch*: The reference square $\hat{S} = (0, 1)^2$ is not further refined. The corresponding triangulation of \hat{S} consists of the single element: $\tilde{\mathcal{T}}^{\text{trivial}} = \{\hat{S}\}$.
2. The *geometric boundary layer patch* $\tilde{\mathcal{T}}_{geo, \sigma}^{\text{BL}, L}$: \hat{S} is refined anisotropically towards $\{\hat{y} = 0\}$ into L elements as depicted in Fig. 2 (top left). The mesh $\tilde{\mathcal{T}}_{geo, \sigma}^{\text{BL}, L}$ is characterized by the nodes $(0, 0)$, $(0, \sigma^i)$, $(1, \sigma^i)$, $i = 0, \dots, L$ and the corresponding rectangular elements generated by these nodes.
3. The *geometric corner patch* $\tilde{\mathcal{T}}_{geo, \sigma}^{\text{C}, n}$: \hat{S} is refined isotropically towards $(0, 0)$ as depicted in Fig. 2 (top middle). Specifically, the reference geometric corner patch mesh $\tilde{\mathcal{T}}_{geo, \sigma}^{\text{C}, n}$ in \hat{S} with geometric refinement towards $(0, 0)$ and n layers is given by triangles determined by the nodes $(0, 0)$, and $(0, \sigma^i)$, $(\sigma^i, 0)$, (σ^i, σ^i) , $i = 0, 1, \dots, n$.
4. The *tensor product patch* $\tilde{\mathcal{T}}_{geo, \sigma}^{\text{T}, L, n}$: \hat{S} is triangulated in $\hat{S}_1 := (0, \sigma^L)^2$ and $\hat{S}_2 := \hat{S} \setminus \hat{S}_1$ separately as depicted in Fig. 2 (bottom left). The triangulation of \hat{S}_1 is a scaled version of $\tilde{\mathcal{T}}_{geo, \sigma}^{\text{C}, n-L}$ characterized by the nodes $(0, 0)$, $(0, \sigma^i)$, $(\sigma^i, 0)$, (σ^i, σ^i) , $i = L, \dots, n$. The triangulation of \hat{S}_2 is characterized by the nodes (σ^i, σ^j) , $i, j = 0, \dots, L$.
5. The *mixed patches* $\tilde{\mathcal{T}}_{geo, \sigma}^{\text{M}, L, n}$: The triangulation consists of both anisotropic elements and isotropic elements as depicted in Fig. 2 (bottom right) and is obtained by triangulating the regions $\hat{S}_1 := (0, \sigma^L)^2$, $\hat{S}_2 := (\hat{S} \setminus \hat{S}_1) \cap \{\hat{y} \leq \hat{x}\}$, $\hat{S}_3 := \hat{S} \setminus (\hat{S}_1 \cup \hat{S}_2)$ separately. \hat{S}_1 is a scaled version of $\tilde{\mathcal{T}}_{geo, \sigma}^{\text{C}, n-L}$ characterized by the nodes $(0, 0)$, $(0, \sigma^i)$, $(\sigma^i, 0)$, (σ^i, σ^i) , $i = L, \dots, n$. The triangulation of \hat{S}_2 is given by the nodes $(\sigma^i, 0)$, (σ^i, σ^j) , $0 \leq i \leq L$, $i \leq j \leq L$ and consists of rectangles and triangles, and only the triangles abutt on the diagonal $\{\hat{x} = \hat{y}\}$. The triangulation of \hat{S}_3 consists of triangles only given by the nodes $(0, \sigma^i)$, (σ^i, σ^i) , $i = 0, \dots, L$.

Remark 3 We kept the list of possible patch refinement patterns in Definition 1 small in order to reduce the number of cases to be discussed for the hp -FE error bounds. A larger number of refinement patterns could facilitate greater flexibility in mesh generation. In particular, the reference patch meshes do not contain general quadrilaterals but only (axiparallel) rectangles; this restriction is not essential but leads to some simplifications in the hp -FE error analysis in [7].

The addition of the diagonal line in the reference corner, tensor, and mixed patches is done to be able to apply the regularity theory of [27] and probably not necessary in actual computations. We also mention that with additional constraints on the macro triangulation $\mathcal{T}^{\mathcal{M}}$ the diagonal line could be dispensed with, [7]. ■

The following definition of the geometric boundary layer mesh $\mathcal{T}_{geo,\sigma}^{L,n}$ formalizes the requirement on the meshes that anisotropic refinement towards $\partial\Omega$ is needed as well as geometric refinement towards the corners.

Definition 2 (geometric boundary layer mesh, [7, Def. 2.3]) Let $\mathcal{T}^{\mathcal{M}}$ be a fixed macro-triangulation consisting of quadrilaterals with analytic element maps that satisfies [27, Def. 2.4.1].

Given $\sigma \in (0, 1)$, $L, n \in \mathbb{N}_0$ with $n \geq L$, a mesh $\mathcal{T}_{geo,\sigma}^{L,n}$ is called a *geometric boundary layer mesh* if the following conditions hold:

1. $\mathcal{T}_{geo,\sigma}^{L,n}$ is obtained by refining each element $K^{\mathcal{M}} \in \mathcal{T}^{\mathcal{M}}$ according to the finite catalog \mathfrak{P} of structured patch-refinement patterns specified in Definition 1, governed by the parameters σ , L , and n .
2. $\mathcal{T}_{geo,\sigma}^{L,n}$ is a regular triangulation of Ω , i.e., it does not have hanging nodes. Since the element maps for the refinement patterns are assumed to be affine, this requirement ensures that the resulting triangulation satisfies [27, Def. 2.4.1].

For each macro-patch $K^{\mathcal{M}} \in \mathcal{T}^{\mathcal{M}}$, exactly one of the following cases is possible:

3. $\overline{K^{\mathcal{M}}} \cap \partial\Omega = \emptyset$. Then the trivial patch is selected as the reference patch.
4. $\overline{K^{\mathcal{M}}} \cap \partial\Omega$ is a single point. Then two cases can occur:
 - (a) $\overline{K^{\mathcal{M}}} \cap \partial\Omega = \{\mathbf{A}_j\}$ for a vertex \mathbf{A}_j of Ω . Then the corresponding reference patch is the corner patch $\tilde{\mathcal{T}}_{geo,\sigma}^{C,n}$ with n layers of refinement towards the origin \mathbf{O} . Additionally, $F_{K^{\mathcal{M}}}(\mathbf{O}) = \mathbf{A}_j$.
 - (b) $\overline{K^{\mathcal{M}}} \cap \partial\Omega = \{\mathbf{P}\}$, where the boundary point \mathbf{P} is not a vertex of Ω . Then the refinement pattern is the corner patch $\tilde{\mathcal{T}}_{geo,\sigma}^{C,L}$ with L layers of geometric mesh refinement towards \mathbf{O} . Additionally, it is assumed that $F_{K^{\mathcal{M}}}(\mathbf{O}) = \mathbf{P} \in \partial\Omega$.
5. $\overline{K^{\mathcal{M}}} \cap \partial\Omega = \bar{e}$ for an edge e of $K^{\mathcal{M}}$ and neither endpoint of e is a vertex of Ω . Then the refinement pattern is the boundary layer patch $\tilde{\mathcal{T}}_{geo,\sigma}^{BL,L}$ and additionally $F_{K^{\mathcal{M}}}(\{\hat{y} = 0\}) \subset \partial\Omega$.
6. $\overline{K^{\mathcal{M}}} \cap \partial\Omega = \bar{e}$ for an edge e of $K^{\mathcal{M}}$ and exactly one endpoint of e is a vertex \mathbf{A}_j of Ω . Then the refinement pattern is the mixed layer patch $\tilde{\mathcal{T}}_{geo,\sigma}^{M,L,n}$ and additionally $F_{K^{\mathcal{M}}}(\{\hat{y} = 0\}) \subset \partial\Omega$ as well as $F_{K^{\mathcal{M}}}(\mathbf{O}) = \mathbf{A}_j$.
7. Exactly two edges of a macro-element $K^{\mathcal{M}}$ are situated on $\partial\Omega$. Then the refinement pattern is the tensor patch $\tilde{\mathcal{T}}_{geo,\sigma}^{T,L,n}$. Additionally, it is assumed that $F_{K^{\mathcal{M}}}(\{\hat{y} = 0\}) \subset \partial\Omega$, $F_{K^{\mathcal{M}}}(\{\hat{x} = 0\}) \subset \partial\Omega$, and $F_{K^{\mathcal{M}}}(\mathbf{O}) = \mathbf{A}_j$ for a vertex \mathbf{A}_j of Ω .

Finally, the following technical condition ensures the existence of certain mesh-lines:

8. For each vertex \mathbf{A}_j of Ω , introduce a set of lines

$$\ell = \bigcup_{K^{\mathcal{M}}: \mathbf{A}_j \in \overline{K^{\mathcal{M}}}} \{ F_{K^{\mathcal{M}}}(\{\hat{y} = 0\}), F_{K^{\mathcal{M}}}(\{\hat{x} = 0\}), F_{K^{\mathcal{M}}}(\{\hat{x} = \hat{y}\}) \}.$$

Let Γ_j, Γ_{j+1} be the two boundary arcs of Ω that meet at \mathbf{A}_j . Then there exists a line $e \in \ell$ such that the interior angles $\angle(e, \Gamma_j)$ and $\angle(e, \Gamma_{j+1})$ are both less than π .

Example 1 Fig. 3 (left and middle) shows an example of an L -shaped domain with macro triangulation and suitable refinement patterns. ■

Remark 4 For fixed L and increasing n , the meshes $\mathcal{T}_{geo,\sigma}^{L,n}$ are geometrically refined towards the vertices of Ω . These meshes are classical geometric meshes for elliptic problems in corner domains as introduced in [4, 5] and discussed in [36, Sec. 4.4.1]. ■

4.2 hp -FE approximation of singularly perturbed problems on geometric boundary layer meshes

The principal result [7, Thm. 4.1] on robust exponential convergence of hp -FEM for (4.1) reads as follows:

Proposition 1 ([7, Thm. 4.1]) *Let $\Omega \subset \mathbb{R}^2$ be a curvilinear polygon with J vertices as described in Section 1.1. Let $A, c \geq c_0 > 0$, f satisfy (4.2). Denote by $\{\mathcal{T}_{geo,\sigma}^{L,n}\}_{L \geq 0, n \geq L}$ a sequence of geometric boundary layer meshes in the sense of Definition 2. Fix $c_1 > 0$.*

Then there are constants $C, b > 0, \beta \in [0, 1)$ (depending solely on the data A, c, f, Ω , on the parameter c_1 , and on the analyticity properties of the patch-maps of the macro-triangulation $\mathcal{T}^{\mathcal{M}}$) such that the following holds: If $\varepsilon \in (0, 1]$ and L satisfy the (boundary layer) scale resolution condition

$$\sigma^L \leq c_1 \varepsilon \tag{4.3}$$

then, for any $q, n \in \mathbb{N}$, the solution $u^\varepsilon \in H_0^1(\Omega)$ of (4.1) can be approximated from $S_0^q(\Omega, \mathcal{T}_{geo,\sigma}^{L,n})$ such that

$$\inf_{v \in S_0^q(\Omega, \mathcal{T}_{geo,\sigma}^{L,n})} (\|u^\varepsilon - v\|_{L^2(\Omega)} + \varepsilon \|\nabla(u^\varepsilon - v)\|_{L^2(\Omega)}) \leq C q^9 \left[\varepsilon^\beta \sigma^{(1-\beta)n} + e^{-bq} \right], \tag{4.4}$$

$$N := \dim S_0^q(\Omega, \mathcal{T}_{geo,\sigma}^{L,n}) \leq C (L^2 q^2 \text{card } \mathcal{T}^{\mathcal{M}} + n q^2 J). \tag{4.5}$$

Proposition 1 is restricted to $\varepsilon \in (0, 1]$. For $\varepsilon \geq 1$, the solution u^ε of (4.1) does not have boundary layer but merely corner singularities. Hence, by Remark 4 meshes with fixed L are appropriate. In particular, the boundary layer scale resolution condition (4.3) is not required:

Proposition 2 Assume the hypotheses on Ω and the data A, c, f as in Proposition 1. Let $\{\mathcal{T}_{geo,\sigma}^{L,n}\}_{L \geq 0, n \geq L}$ be a sequence of geometric boundary layer meshes².

There are constants $C, b > 0, \beta \in [0, 1)$ (depending solely on $A, c, f, \sigma \in (0, 1)$, and the analyticity properties of the macro-triangulation) such that the solution u^ε of (4.1) satisfies

$$\forall L, n \in \mathbb{N}_0, q \in \mathbb{N}: \inf_{v \in S_0^q(\Omega, \mathcal{T}_{geo,\sigma}^{L,n})} \|u^\varepsilon - v\|_{H^1(\Omega)} \leq C\varepsilon^{-2} q^9 \left(\sigma^{(1-\beta)n} + e^{-bq} \right), \quad (4.6)$$

and $\dim S_0^q(\Omega, \mathcal{T}_{geo,\sigma}^{L,n})$ satisfies (4.5).

4.3 hp -FE approximation of singularly perturbed problems on admissible meshes $\mathcal{T}_{min,\lambda}^{L,q}(\varepsilon)$ in Ω

In Proposition 1, the solution u^ε is approximated on patchwise geometric meshes. These meshes are able to capture boundary layers (and corner layers) on a whole range of singular perturbation parameters ε : as long as a lower bound for ε is known and provided that geometric mesh refinement resolves all scales, robust exponential convergence is assured.

On the other hand, if there is a single, explicitly known scale ε then the “minimal, admissible boundary layer meshes” $\mathcal{T}_{min,\lambda}^{L,q}(\varepsilon) := \mathcal{T}(\min\{\kappa_0, \lambda p\varepsilon\}, L)$ of [27, Def. 2.4.4] (see also [38, Fig. 11] or [30, Fig. 2]), which are designed to resolve a single, explicitly known length scale with hp -FEM may be employed. In contrast to the geometric boundary layer meshes of Def. 2, these “minimal” boundary-fitted meshes are ε -dependent.

Proposition 3 ([27, Thm. 2.4.8 in conjunction with Thm. 3.4.8]) Let $\Omega \subset \mathbb{R}^2$ be a curvilinear polygon with J vertices as described in Section 1.1. Let $A, c \geq c_0 > 0, f$ satisfy (4.2).

Consider, for $\kappa_0 > 0$ determined by Ω , the two-parameter family $\mathcal{T}(\kappa, L), (\kappa, L) \in (0, \kappa_0] \times \mathbb{N}$, of admissible meshes in the sense of [27, Def. 2.4.4], [17, Def. 3.1, Figs. 1, 2]. Let u^ε be the solution of (4.1).

Then there are constants b, λ_0 independent of $\varepsilon \in (0, 1]$ such that for every $\lambda \in (0, \lambda_0]$ there is $C > 0$ such that for every $q \geq 1, L \geq 0$ there holds the error bounds

$$\inf_{v \in S_0^q(\Omega, \mathcal{T}_{min,\lambda}^{L,q}(\varepsilon))} \|u^\varepsilon - v\|_{L^2(\Omega)} + \varepsilon \|\nabla(u^\varepsilon - v)\|_{L^2(\Omega)} \leq Cq^6 [e^{-b\lambda q} + \varepsilon e^{-bL}], \quad (4.7)$$

$$\mathcal{T}_{min,\lambda}^{L,q}(\varepsilon) := \mathcal{T}(\min\{\kappa_0, \lambda q\varepsilon\}, L), \quad (4.8)$$

$$N := \dim S_0^q(\Omega, \mathcal{T}_{min,\lambda}^{L,q}(\varepsilon)) \leq CLq^2. \quad (4.9)$$

² No boundary layer refinement/ resolution is required here, i.e., “ordinary”, corner refined geometric mesh sequences will suffice.

In particular, for $L \sim q$, one has with C, b' independent of ε

$$\inf_{v \in S_0^q(\Omega, \mathcal{T}_{min,\lambda}^{L,q}(\varepsilon))} \|u^\varepsilon - v\|_{L^2(\Omega)} + \varepsilon \|\nabla(u^\varepsilon - v)\|_{L^2(\Omega)} \leq C \exp(-b' N^{1/3}).$$

For $\varepsilon \geq 1$ these admissible boundary layer meshes are the well-known geometric meshes with L layers of geometric refinement as introduced in [4, 5] and discussed in [36, Sec. 4.4.1]. These geometric, corner-refined meshes are similar to the meshes $\mathcal{T}_{geo,\sigma}^{L,n}$ with fixed $L = 0$ discussed in Remark 4. In particular, the minimal boundary layer meshes $\mathcal{T}_{min,\lambda}^{L,q}(\varepsilon)$ for $\varepsilon \geq 1$ do not really depend on ε , λ , and q . However, for consistency of notation, we keep the notation $\mathcal{T}_{min,\lambda}^{L,q}(\varepsilon)$ in the following result, which covers the case $\varepsilon \geq 1$. We need this result since the range (3.8) of eigenvalues μ_i involves also eigenvalues $\mu_i \geq 1$.

Proposition 4 *Under the assumptions of Proposition 3, there exist constants $b, C > 0$ such that*

$$\forall \varepsilon \geq 1, \forall q, L \in \mathbb{N} : \inf_{v \in S_0^q(\mathcal{T}_{min,\lambda}^{L,q}(\varepsilon))} \|u^\varepsilon - v\|_{H^1(\Omega)} \leq C \varepsilon^{-2} q^6 [e^{-b\lambda q} + e^{-bL}],$$

$$\text{where } N := \dim S_0^q(\Omega, \mathcal{T}_{min,\lambda}^{L,q}(\varepsilon)) \leq CLq^2.$$

In particular, for $L \sim q$, there are constants $b', C > 0$ such that

$$\forall \varepsilon \geq 1, q, L \in \mathbb{N} : \inf_{v \in S_0^q(\Omega, \mathcal{T}_{min,\lambda}^{L,q}(\varepsilon))} \|u^\varepsilon - v\|_{H^1(\Omega)} \leq C \varepsilon^{-2} \exp(-b' N^{1/3}).$$

It is worth pointing out the following differences between the approximation on geometric boundary layer meshes $\mathcal{T}_{geo,\sigma}^{L,n}$ and on the minimal admissible boundary layer meshes $\mathcal{T}_{min,\lambda}^{L,q}$: a) the use of the mesh $\mathcal{T}_{geo,\sigma}^{L,n}$ requires the scale resolution condition (4.3). It requires $L \gtrsim |\ln \varepsilon|$ so that the approximation result Proposition 1 depends (weakly) on ε . b) Selecting $n \simeq L \simeq q$ in Proposition 1 yields convergence $O(\exp(-b\sqrt[4]{N}))$ whereas the choice $L \simeq q$ in Proposition 3 yields the better convergence behavior $O(\exp(-b'\sqrt[3]{N}))$. c) The meshes $\mathcal{T}_{min,\lambda}^{L,q}$ are designed to approximate a *single* scale well whereas the meshes $\mathcal{T}_{geo,\sigma}^{L,n}$ are capable to resolve a range of scales. d) The meshes $\mathcal{T}_{min,\lambda}^{L,q}$ rely on a suitable choice of the parameter λ whereas the geometric boundary layer meshes $\mathcal{T}_{geo,\sigma}^{L,n}$ do not have parameters that need to be suitably chosen.

5 Exponential Convergence of Extended hp -FEM

Based on the hp semidiscretization in the extended variable combined with the diagonalization in Section 3, we use the hp -approximation results from Section 4 to prove exponential convergence of hp -FEM for the CS-extended problem (1.14).

As is revealed by the diagonalization (3.5), the y -semidiscrete solution $G_M^{\mathcal{T}} \mathcal{U}$ contains \mathcal{M} separate length scales associated with the eigenvalues μ_i , $i = 1, \dots, \mathcal{M}$. The solutions $U_i \in H_0^1(\Omega)$ of the resulting \mathcal{M} many independent,

linear second-order reaction-diffusion problems in Ω exhibit both, boundary layers and corner singularities.

In **Case A**, which we discuss in Section 5.1, we employ for each i a “minimal” hp -FE space in Ω that resolves boundary- and corner layers appearing in the U_i due to possibly large/small values of μ_i . Mesh design principles for such “minimal” FE spaces that may resolve a single scale of a singularly perturbed problem have already been presented in, e.g., [25, 27, 28, 37, 38]; the specific choice $\mathcal{T}_{min,\lambda}^{L,q}(\varepsilon)$ has been discussed in Propositions 3, 4 and will be used in our analysis.

In **Case B**, which we discuss in Section 5.2, we discretize these decoupled, reaction-diffusion problems by *one common hp -FEM in the bounded polygon Ω* , which employs both, geometric corner refinement as well as geometric boundary refinement, as in [27, 28]. Due to the need to obtain FE solutions for *all* μ_i in *one common FE space in Ω* , however (in order that the sum (3.13) belong to a tensor product hp -FE space), our analysis will provide *one hp -FE space in Ω* which will resolve *all* boundary and corner layers due to small parameters μ_i near $\partial\Omega$. As we shall show, in **Case B** the total number of DOFs is larger than in **Case A**.

5.1 Exponential Convergence I: Diagonalization and Minimal Meshes

The robust exponential convergence result Proposition 3 allows us to establish, in conjunction with the diagonalization (3.2)–(3.4), a first exponential convergence result in **Case A** of Section 3. We consider the following numerical scheme, which relies on the “minimal boundary layer meshes” $\mathcal{T}_{min,\lambda}^{L,q}(\varepsilon)$ from [27, Sec. 2.4.2] already discussed in Proposition 3:

- (1) Select \mathcal{Y} with $c_1 M \leq \mathcal{Y} \leq c_2 M$ and consider the space $S_{\{\mathcal{Y}\}}^{\mathbf{r}}((0, \mathcal{Y}), \mathcal{G}_{geo,\sigma}^M)$ for the geometric mesh $\mathcal{G}_{geo,\sigma}^M$ on $(0, \mathcal{Y})$ with M elements and a linear degree vector \mathbf{r} with slope $\mathfrak{s} > 0$.
- (2) Solve the eigenvalue problem (3.2), (3.3).
- (3) Select $\lambda > 0$. Define $U_i^{q,L} \in S_0^q(\mathcal{T}_{min,\lambda}^{L,q}(\sqrt{\mu_i}))$ as the solution of

$$\forall v \in S_0^q(\mathcal{T}_{min,\lambda}^{L,q}(\sqrt{\mu_i})) : a_{\mu_i,\Omega}(U_i^{q,L}, v) = d_s v_i(0) \langle f, v \rangle. \quad (5.1)$$

- (4) Define the approximation $\mathcal{U}^{q,L}(x, y) := \sum_{i=1}^{\mathcal{M}_{geo}} v_i(y) U_i^{q,L}(x)$.

For the approximation error $\mathcal{U} - \mathcal{U}^{q,L}$ we have:

Theorem 1 *Let $\Omega \subset \mathbb{R}^2$ be a curvilinear polygon with J vertices as described in Section 1.1. Let A, f satisfy (1.1) and let A be uniformly symmetric positive definite on Ω . Fix positive constants c_1, c_2 , and \mathfrak{s} .*

Then there are constants $C, b, b', \lambda_0 > 0$ (depending on Ω, A, c , and the parameters characterizing the mesh family $\mathcal{T}_{min,\lambda}^{L,q}$) such that for any $\lambda \in (0, \lambda_0]$ there holds for all $q, M \geq 1, L \geq 0$

$$\begin{aligned} \|u - \text{tr}_\Omega \mathcal{U}^{q,L}\|_{\mathbb{H}^s(\Omega)} &\lesssim \|\nabla(\mathcal{U} - \mathcal{U}^{q,L})\|_{L^2(y^\alpha, C)} \\ &\leq CM^{2-\alpha} q^6 [\exp(-b\lambda q) + \exp(-b'L)] + \exp(-b''M). \end{aligned} \quad (5.2)$$

In particular, for $q \simeq L \simeq M \simeq p$, denoting $\mathcal{U}^p := \mathcal{U}^{q,L}$ with this choice of q and L , and the total number of degrees of freedom $N = \sum_i \dim S_0^q(\Omega, \mathcal{T}_{min,\lambda}^{L,q}(\sqrt{\mu_i}))$,

$$\|u - \text{tr}_\Omega \mathcal{U}^p\|_{\mathbb{H}^s(\Omega)} \lesssim \|\nabla(\mathcal{U} - \mathcal{U}^p)\|_{L^2(y^\alpha, \mathcal{C})} \lesssim \exp(-bp) \simeq \exp(-b''' \sqrt[5]{N}), \quad (5.3)$$

where the constant b''' depends additionally on the implied constants in $q \simeq L \simeq M$.

Remark 5 The approximation result (5.3) still holds if the linear degree vector \mathbf{r} in the definition of $\mathcal{U}^{q,L}$ is replaced with a constant polynomial degree $r \sim M$. ■

Proof Step 1 (semidiscretization error): The analyticity of f on $\overline{\Omega}$ implies $f \in \mathbb{H}^{-s+\nu}(\Omega)$ for any $\nu \in (0, 1/2 + s)$. Hence, by (3.1), the semidiscretization error $\mathcal{U} - G_M^{\mathbf{r}} \mathcal{U}$ satisfies for suitable $b > 0$ independent of M

$$\|\mathcal{U} - G_M^{\mathbf{r}} \mathcal{U}\|_{\mathcal{C}} \lesssim e^{-bM}. \quad (5.4)$$

Step 2 (representation of $G_M^{\mathbf{r}} \mathcal{U}$): The semidiscrete approximation $G_M^{\mathbf{r}} \mathcal{U}$ may be expressed in terms of the eigenbasis $\{v_j\}_{j=1}^M$ in (3.2), (3.3) as

$$(G_M^{\mathbf{r}} \mathcal{U})(x', y) = \sum_{i=1}^{\mathcal{M}_{geo}} v_i(y) U_i(x'),$$

where the function U_i solve by (3.5)

$$\forall V \in H_0^1(\Omega) : a_{\mu_i, \Omega}(U_i, V) = d_s v_i(0) \langle f, V \rangle.$$

Step 3: For every $i = 1, \dots, \mathcal{M}_{geo}$, and for every $q \in \mathbb{N}$, approximate the $U_i \in H_0^1(\Omega)$ by its Galerkin approximation $U_i^{q,L} \in S_0^q(\Omega, \mathcal{T}_{min,\lambda}^{L,q}(\sqrt{\mu_i})) \subset H_0^1(\Omega)$. That is, $U_i^{q,L} = \Pi_i^q U_i$ is the $a_{\mu_i, \Omega}(\cdot, \cdot)$ -projection of U_i given by (3.9). It is the best approximation to U_i in the corresponding energy norm and satisfies

$$\|U_i - \Pi_i^q U_i\|_{\mu_i, \Omega} = \min_{V \in S_0^q(\Omega, \mathcal{T}_{min,\lambda}^{L,q}(\sqrt{\mu_i}))} \|U_i - V\|_{\mu_i, \Omega}.$$

By linearity of Π_i^q and the analyticity of f Propositions 3, 4 (depending on whether $\mu_i \leq 1$ or $\mu_i > 1$) and Lemma 2

$$\|U_i - \Pi_i^q U_i\|_{\mu_i, \Omega} \lesssim |v_i(0)| q^6 \left(e^{-b\lambda q} + \sqrt{\mu_i} e^{-b'L} \right) \lesssim \mathcal{M}_{geo}^{(1-\alpha)/2} q^6 \left(e^{-b\lambda q} + \sqrt{\mu_i} e^{-b'L} \right).$$

Step 4 (Proof of (5.2)): With the approximations $U_i^{q,L}$ the approximation $\mathcal{U}^{q,L}$ of \mathcal{U} is given by

$$\mathcal{U}^{q,L}(x', y) := \sum_{i=1}^{\mathcal{M}_{geo}} v_i(y) U_i^{q,L}(x') \in \mathring{H}^1(y^\alpha, \mathcal{C}).$$

From (3.7) we get for $Z = \mathcal{U}_M - \mathcal{U}^{q,L} = \sum_{i=1}^{\mathcal{M}_{geo}} v_i(y)(U_i(x) - U_i^{q,L}(x))$

$$\|Z\|_{\mathcal{C}}^2 = a_{\mathcal{C}}(Z, Z) = \sum_{i=1}^{\mathcal{M}_{geo}} \|U_i - U_i^q\|_{\mu_i, \Omega}^2 \lesssim \mathcal{M}_{geo}^{2-\alpha} q^{12} [\exp(-2b\lambda q) + \exp(-2b'L)] .$$

We note that $\mathcal{M}_{geo} \sim M^2$. Combining this last estimate with (5.4) yields the second estimate in (5.2). The first estimate in (5.2) expresses the continuity of the trace operator at $y = 0$.

Step 5 (complexity estimate): Using that $\mathcal{M}_{geo} = O(M^2) = O(q^2)$ and the fact that $\dim S_0^q(\Omega, \mathcal{T}_{min, \lambda}^{L, q}(\sqrt{\mu_i})) \leq CLq^2 = O(q^3)$ as well as the assumption $q \simeq L \simeq M \simeq p$, we arrive at a total problem size $N = O(q^5)$. Absorbing algebraic factors in the exponentially decaying one in (5.2) then yields (5.3).

5.2 Exponential Convergence II: Geometric Boundary Layer Meshes

In this section, we show that exponential convergence of a Galerkin method for (1.14) can be achieved by a suitable choice of meshes \mathcal{T} and \mathcal{G}^M in the tensor product space $\mathbb{V}_{h, M}^{q, \mathbf{r}}(\mathcal{T}, \mathcal{G}^M)$ of (2.6). That is, we place ourselves in **Case B** in Section 3.2. For the discretization in y , we select again the spaces $S_{\{\mathcal{Y}\}}^{\mathbf{r}}((0, \mathcal{Y}), \mathcal{G}_{geo, \sigma}^M)$ with $\mathcal{Y} \sim M$ and the linear degree vector \mathbf{r} with slope \mathfrak{s} . The hp -FE discretization in Ω is based on the space $S_0^q(\Omega, \mathcal{T}_{geo, \sigma}^{L, n})$ with the geometric boundary layer mesh $\mathcal{T}_{geo, \sigma}^{L, n}$ in Definition 2. Recall that $G_{h, M}^{q, \mathbf{r}} \mathcal{U}$ denotes the Galerkin projection of the solution \mathcal{U} onto $\mathbb{V}_{h, M}^{q, \mathbf{r}}(\mathcal{T}_{geo, \sigma}^{L, n}, \mathcal{G}_{geo, \sigma}^M) = S_0^q(\Omega, \mathcal{T}_{geo, \sigma}^{L, n}) \otimes S_{\{\mathcal{Y}\}}^{\mathbf{r}}((0, \mathcal{Y}), \mathcal{G}_{geo, \sigma}^M)$. In Theorem 2 below, we will focus on the case $q \simeq L \simeq M$ and the corresponding Galerkin projection is denoted \mathcal{U}_{TP}^p .

- Remark 6* (i) In contrast to the procedure of **Case A** in the preceeding Section 5.1, precise knowledge of the length scales $\sqrt{\mu_i}$ is not necessary.
(ii) The diagonalization procedure may be carried out numerically and results in decoupled reaction-diffusion problems, affording parallel numerical solution.
(iii) The linear degree vector \mathbf{r} could be replaced with a constant degree $r \sim M$, and Theorem 2 will still hold. ■

For the tensor-product hp -FEM in $\mathcal{C}_{\mathcal{Y}}$ we also have an exponential convergence result:

Theorem 2 *Let $\Omega \subset \mathbb{R}^2$ be a curvilinear polygon with J vertices as described in Section 1.1. Let A, f satisfy (1.1) and let A be uniformly symmetric positive definite on Ω . Fix a slope $\mathfrak{s} > 0$. Set*

$$\mathcal{Y} \simeq L \simeq M \simeq n \simeq q =: p \tag{5.5}$$

With these choices, denote by \mathcal{U}_{TP}^p the Galerkin projection of \mathcal{U} onto the tensor product hp -FE space $\mathbb{V}_{h, M}^{q, \mathbf{r}}(\mathcal{T}_{geo, \sigma}^{L, n}, \mathcal{G}_{geo, \sigma}^M) = S_0^q(\Omega, \mathcal{T}_{geo, \sigma}^{L, n}) \otimes S_{\{\mathcal{Y}\}}^{\mathbf{r}}((0, \mathcal{Y}), \mathcal{G}_{geo, \sigma}^M)$.

Then $N := \dim \mathbb{V}_{h,M}^{q,r}(\mathcal{T}_{geo,\sigma}^{L,n}, \mathcal{G}_{geo,\sigma}^M) = O(p^6)$ and there are constants $C, b, b' > 0$ depending only on Ω, A, f , the macro triangulation \mathcal{T}^M underlying the geometric boundary layer meshes $\mathcal{T}_{geo,\sigma}^{L,n}$, the slope \mathfrak{s} , and the implied constants in (5.5) such that

$$\|u - \text{tr}_\Omega \mathcal{U}_{TP}^p\|_{\mathbb{H}^s(\Omega)} \lesssim \|\nabla(\mathcal{U} - \mathcal{U}_{TP}^p)\|_{L^2(y^\alpha, \mathcal{C})} \lesssim \exp(-bp) \simeq \exp(-b' \sqrt[6]{N}).$$

Proof The proof of this result is structurally along the lines of the proof of Theorem 1. We omit details and merely indicate how the scale resolution condition (4.3) is now accounted for. We note that for fixed \mathcal{Y} and $M' < M$, we have that the spaces $S_{\{\mathcal{Y}\}}^r((0, \mathcal{Y}), \mathcal{G}^{M'})$ and $S_{\{\mathcal{Y}\}}^r((0, \mathcal{Y}), \mathcal{G}_{geo,\sigma}^M)$ satisfy $S_{\{\mathcal{Y}\}}^r((0, \mathcal{Y}), \mathcal{G}_{geo,\sigma}^{M'}) \subset S_{\{\mathcal{Y}\}}^r((0, \mathcal{Y}), \mathcal{G}_{geo,\sigma}^M)$ (if the same slope \mathfrak{s} for the linear degree vector is chosen). Hence, the Galerkin error for the approximation from the space $S_0^q(\Omega, \mathcal{T}_{geo,\sigma}^{L,n}) \otimes S_{\{\mathcal{Y}\}}^r((0, \mathcal{Y}), \mathcal{G}_{geo,\sigma}^M)$ is smaller than that from $S_0^q(\Omega, \mathcal{T}_{geo,\sigma}^{L,n}) \otimes S_{\{\mathcal{Y}\}}^r((0, \mathcal{Y}), \mathcal{G}_{geo,\sigma}^{M'})$, and we therefore focus on bounding the approximation error for $S_0^q(\Omega, \mathcal{T}_{geo,\sigma}^{L,n}) \otimes S_{\{\mathcal{Y}\}}^r((0, \mathcal{Y}), \mathcal{G}_{geo,\sigma}^{M'})$. We select M' of the form $M' = \lfloor \eta M \rfloor$ for some η to be chosen below. For ease of notation, we simply set $M' = \eta M$.

By Lemma 2 we have that the smallest length scale of the singularly perturbed problems for the space $S_0^q(\mathcal{T}_{geo,\sigma}^{L,n}) \otimes S_{\{\mathcal{Y}\}}^r(\mathcal{G}_{geo,\sigma}^{M'})$ is $\min_i \mu_i \gtrsim M'^{-2} \sigma^{2M'}$ and that scale resolution condition (4.3) therefore reads

$$\sigma^L \leq c_1 \min_i \sqrt{\mu_i} \leq c_1 M'^{-1} \sigma^{M'} \leq c_1 \eta M^{-1} \sigma^{\eta M} \quad (5.6)$$

Since $L \simeq M$, we see that (5.6) can be satisfied for some fixed c_1 provided η is suitably chosen. The approximation of \mathcal{U} from $S_0^q(\mathcal{T}_{geo,\sigma}^{L,n}) \otimes S_{\{\mathcal{Y}\}}^r(\mathcal{G}_{geo,\sigma}^{M'})$ then follows by arguments very similar to those of the proof of Theorem 1.

6 Exponential Convergence of sinc BK-FEM

The hp -sinc BK FEM is based on exponentially convergence, so-called “sinc” quadratures to the Balakrishnan formula

$$\mathcal{L}^{-s} = c_B \int_{-\infty}^{\infty} e^{-sy} (I + e^{-y} \mathcal{L})^{-1} dy. \quad (6.1)$$

as described in Section 1.5 and (1.15) (see [9–11] and the references there). We briefly review the corresponding exponential convergence results in Section 6.1. The numerical realization of the sinc quadrature approximation of (6.1) leads again to the numerical solution of decoupled, local linear reaction-diffusion problems in Ω . These boundary value problems are again singularly perturbed. Accordingly, we discuss two classes of hp -FE approximations for their numerical solution: In Section 6.2.1, we discuss **Case A**, which is based on the *minimal boundary layer meshes* $\mathcal{T}_{min,\lambda}^{L,q}$ in Ω . In Section 6.2.2, we detail **Case B**, where *geometric boundary layer meshes* in Ω are employed. The latter allow one common hp -FEM for all values of parameters arising from the sinc quadrature approximation of (6.1).

6.1 Sinc quadrature approximation

The above integral (6.1) can be discretized by so-called “sinc” quadratures (see, e.g., [9, 39]). To that end, we define for $K \in \mathbb{N}$

$$y_j := jK^{-1/2} = jk, \quad |j| \leq K, \quad k := 1/\sqrt{K}. \quad (6.2)$$

For $f \in L^2(\Omega) \subset \mathbb{H}^{-s}(\Omega)$ for every $0 < s < 1$, the (semidiscrete) *sinc quadrature approximation* u_M of $u = \mathcal{L}^{-s}f \in \mathbb{H}^s(\Omega)$ as represented in (6.1) reads with $\varepsilon_j := e^{-y_j/2} = e^{j/(2\sqrt{K})}$, $|j| \leq K$:

$$u_K = Q_k^{-s}(\mathcal{L})f := c_B k \sum_{|j| \leq K} \varepsilon_j^{2s} (I + \varepsilon_j^2 \mathcal{L})^{-1} f. \quad (6.3)$$

We note that for any k , we have that $Q_k^{-s}(\mathcal{L}) : \mathbb{H}^{-1}(\Omega) \rightarrow \mathbb{H}^1(\Omega)$ is a bounded linear map. By the continuous embeddings $\mathbb{H}^1(\Omega) \subseteq \mathbb{H}^s(\Omega) \subseteq \mathbb{H}^{-s}(\Omega) \subseteq \mathbb{H}^{-1}(\Omega)$, also $Q_k^{-s}(\mathcal{L}) : \mathbb{H}^{-s}(\Omega) \rightarrow \mathbb{H}^s(\Omega)$ is a bounded linear map for any $0 < s < 1$. The semidiscretization error $\mathcal{L}^{-s} - Q_k^{-s}(\mathcal{L})$ is bound in [9]:

Proposition 5 ([9, Thm. 3.2]) *For $f \in L^2(\Omega)$ and for every $0 \leq \beta < s$ with $0 < s < 1$ denoting the exponent of the fractional diffusion operator in (1.4), there exist constants $b, C > 0$ (depending on β, s, Ω , and \mathcal{L}) such that for every $k > 0$ as in (6.2) holds, with $D(\mathcal{L}^\beta) = \mathbb{H}^{2\beta}(\Omega)$ where $\mathbb{H}^\sigma(\Omega)$ is as in (1.3),*

$$\|(\mathcal{L}^{-s} - Q_k^{-s}(\mathcal{L}))f\|_{D(\mathcal{L}^\beta)} \leq C \exp(-b/k) \|f\|_{L^2(\Omega)}. \quad (6.4)$$

Remark 7 Sinc approximation formulas such as (6.3) have a number of parameters which can be optimized in various ways. The error bound in Proposition 5 is merely one particular choice (the so-called “balanced” choice of parameters), which is sufficient for the exponential sinc error bound (6.4). Other choices yield analogous (exponential) sinc error bounds, with possibly better numerical values for the constants $b, C > 0$ in (6.4). We point out that we make such a choice in our numerical examples in (7.3) and refer to [9, Rem. 3.1] for details. ■

6.2 hp -FE approximation in Ω

The sinc approximation error bound (6.4) implies exponential convergence of the sinc quadrature sum (6.3), which we write as

$$Q_k^{-s}(\mathcal{L})f = c_B k \sum_{|j| \leq K} \varepsilon_j^{2s} w_j. \quad (6.5)$$

Here, the $w_j \in H_0^1(\Omega)$ are solutions of the $2K + 1$ reaction-diffusion problems

$$\varepsilon_j^2 \mathcal{L} w_j + w_j = f \quad \text{in } \Omega, \quad w_j|_{\partial\Omega} = 0, \quad |j| \leq K. \quad (6.6)$$

With the bilinear form $a_{\varepsilon_j^2, \Omega}(\cdot, \cdot)$ from (3.6), their variational formulations reads: find $w_j \in H_0^1(\Omega)$ such that

$$\forall v \in H_0^1(\Omega) : a_{\varepsilon_j^2, \Omega}(w_j, v) = (f, v) . \quad (6.7)$$

The reaction diffusion problems (6.6) are again of the type (3.5) for which exponentially convergent *hp*-FE approximations were presented in Section 5, from [27] and [7]. A *fully discrete sinc BK-FEM approximation* is constructed by replacing w_j in (6.5), (6.6) by one of the *hp*-FE approximations discussed in Section 5. As in the case of the Extended *hp*-FEM, also for the sinc BK-FEM one can distinguish **Case A**, in which each problem (6.7) is discretized using a different *hp*-FE space, and **Case B**, where all problems (6.7) are discretized by the same *hp*-FE space in Ω .

6.2.1 Case A

We discretize the singularly perturbed problems (6.7) with length scales ε_j using the spaces $\mathcal{T}_{min, \lambda}^{L, q}(\varepsilon_j)$. That is, denoting the resulting approximations generically by w_j^{hp} , defined by: for $|j| \leq K$, find $w_j^{hp} \in S_0^q(\Omega, \mathcal{T}_{min, \lambda}^{L, q}(\varepsilon_j))$ such that

$$\forall v \in S_0^q(\Omega, \mathcal{T}_{min, \lambda}^{L, q}(\varepsilon_j)) : a_{\varepsilon_j^2, \Omega}(w_j^{hp}, v) = \langle f, v \rangle . \quad (6.8)$$

The *hp*-FE approximations w_j^{hp} are well-defined. Replacing in (6.5) the w_j by their *hp*-FE approximations, we obtain the sinc BK-FEM approximation of the (inverse of) the fractional diffusion operator \mathcal{L}^s :

$$Q_k^{-s}(\mathcal{L}_{hp})f := c_B k \sum_{|j| \leq K} \varepsilon_j^{2s} w_j^{hp} . \quad (6.9)$$

To bound the error $\|u - Q_k^{-s}(\mathcal{L}_{hp})f\|_{\mathbb{H}^s(\Omega)}$, we write

$$\|u - Q_k^{-s}(\mathcal{L}_{hp})f\|_{\mathbb{H}^s(\Omega)} \leq \|(\mathcal{L}^{-s} - Q_k^{-s}(\mathcal{L}))f\|_{\mathbb{H}^s(\Omega)} + \|Q_k^{-s}(\mathcal{L} - \mathcal{L}_{hp})f\|_{\mathbb{H}^s(\Omega)} .$$

For the first term, the sinc approximation error, we use the error bound (6.4) with $\beta = s/2$. Using $D(\mathcal{L}^{s/2}) = \mathbb{H}^s(\Omega)$ for $0 < s < 1$, we obtain from (6.4) and from $k \simeq K^{-1/2}$ (see (6.2)) the bound

$$\|(\mathcal{L}^{-s} - Q_k^{-s}(\mathcal{L}))f\|_{\mathbb{H}^s(\Omega)} \leq C \exp(-b\sqrt{K}) \|f\|_{L^2(\Omega)} . \quad (6.10)$$

To bound the second term, definition (6.5) and the triangle inequality imply

$$\|Q_k^{-s}(\mathcal{L} - \mathcal{L}_{hp})f\|_{\mathbb{H}^s(\Omega)} \lesssim k \sum_{|j| \leq K} \varepsilon_j^{2s} \|w_j - w_j^{hp}\|_{\mathbb{H}^s(\Omega)} . \quad (6.11)$$

To invoke the *hp*-error bound (4.4) with the norm (3.7), we use the interpolation inequality

$$\forall 0 < s < 1 \exists C_s > 0 \forall w \in H_0^1(\Omega) : \|w\|_{\mathbb{H}^s(\Omega)} \leq C_s \|w\|_{L^2(\Omega)}^{1-s} \|\nabla w\|_{L^2(\Omega)}^s . \quad (6.12)$$

We apply this to each term in (6.11) and, using the definition (3.7) of the norm $\|w\|_{\varepsilon^2, \Omega}$, and $\|w\|_{\varepsilon^2}^2 := \varepsilon^2 \|\nabla w\|_{L^2(\Omega)}^2 + \|w\|_{L^2(\Omega)}^2 \simeq (\varepsilon \|\nabla w\|_{L^2(\Omega)} + \|w\|_{L^2(\Omega)})^2$ for all $\varepsilon \geq 0$, arrive at

$$\begin{aligned} \|Q_k^{-s}(\mathcal{L} - \mathcal{L}_{hp})f\|_{\mathbb{H}^s(\Omega)} &\lesssim k \sum_{|j| \leq K} \varepsilon_j^s \|w_j - w_j^{hp}\|_{L^2(\Omega)}^{1-s} \left(\varepsilon_j \|\nabla(w_j - w_j^{hp})\|_{L^2(\Omega)} \right)^s \\ &\lesssim k \sum_{|j| \leq K} \varepsilon_j^s \|w_j - w_j^{hp}\|_{\varepsilon_j^2}^2. \end{aligned}$$

We split the summation indices as $I_+ \cup I_-$, i.e., $I_+ := \{|j| \leq K\} \cap \{j > 0\}$ and $I_- := \{|j| \leq K\} \cap \{j \leq 0\}$.

As $\varepsilon_j = \exp(j/(2\sqrt{K}))$, $j \in I_-$ implies $0 < \varepsilon_j \leq 1$ and $j \in I_+$ to $1 < \varepsilon_j \leq \exp(\sqrt{K}/2)$. With Proposition 4, we estimate the sum over $j \in I_+$ according to

$$\begin{aligned} \sum_{j \in I_+} \varepsilon_j^s \|w_j - w_j^{hp}\|_{\varepsilon_j^2}^2 &\lesssim q^6 \sum_{j \in I_+} \varepsilon_j^{s-1} (\exp(-bq) + \exp(-b'L)) \\ &= q^6 (\exp(-bq) + \exp(-b'L)) \sum_{j \in I_+} \exp(j(s-1)/(2\sqrt{K})) \\ &\lesssim \sqrt{K} q^6 (\exp(-bq) + \exp(-b'L)). \end{aligned} \quad (6.13)$$

We estimate the sum over $j \in I_-$ (i.e., $0 < \varepsilon_j \leq 1$) with Proposition 3

$$\begin{aligned} \sum_{j \in I_-} \varepsilon_j^s \|w_j - w_j^{hp}\|_{\varepsilon_j^2}^2 &\lesssim q^6 \sum_{j \in I_-} \varepsilon_j^s [\exp(-b\lambda q) + \varepsilon_j \exp(-b'L)] \\ &\lesssim q^6 [\exp(-b\lambda q) + \exp(-b'L)] \sum_{j=1}^K \exp(-sj/(2\sqrt{K})) \\ &\simeq \sqrt{K} q^6 [\exp(-b\lambda q) + \exp(-b'L)]. \end{aligned} \quad (6.14)$$

We select $L \simeq q$ (i.e., the number L of mesh-layers proportional to the polynomial degree $q \geq 1$) with proportionality constant independent of ε_j . Furthermore, we note $k = 1/\sqrt{K}$ and select $K \simeq q$ so that

$$\|Q_k^{-s}(\mathcal{L} - \mathcal{L}_{hp})f\|_{\mathbb{H}^s(\Omega)} \lesssim q^6 \exp(-b\lambda q). \quad (6.15)$$

Combining the error bounds (6.10) and (6.15), and suitably adjusting the constant $b > 0$ in the exponential bounds, we arrive at

$$\|u - Q_k^{-s}(\mathcal{L}_{hp})f\|_{\mathbb{H}^s(\Omega)} \lesssim \exp(-bq). \quad (6.16)$$

Given that the approximation $u_{K,hp}$ involves the solution of $O(K) = O(q^2)$ reaction-diffusion problems, each of which requires $O(q^3)$ DOF, the error bound (6.16) in terms of the total number of degrees of freedom N_{DOF} reads

$$\|u - Q_k^{-s}(\mathcal{L}_{hp})f\|_{\mathbb{H}^s(\Omega)} \leq C \exp(-b\sqrt[5]{N_{DOF}}) \quad (6.17)$$

with constants $b, C > 0$ that are independent of N_{DOF} . We have thus shown:

Theorem 3 *Let Ω be a curvilinear polygon as defined in Section 1.1, let A, f satisfy (1.1), and let A be uniformly symmetric positive definite on Ω . Let u be the solution to (1.4), and let its fully discrete approximation be given by the sinc BK-FEM approximation (6.5) in conjunction with the hp-FE approximation of w_j^{hp} in (6.8) with the hp-FE spaces $S_0^q(\Omega, \mathcal{T}_{min,\lambda}^{L,q}(\varepsilon_j))$ on the minimal boundary layer meshes $\mathcal{T}_{min,\lambda}^{L,q}(\varepsilon_j)$. Choose further the parameters $q \simeq L \simeq K$ and let $N = \sum_{|j| \leq K} \dim S_0^q(\Omega, \mathcal{T}_{min,\lambda}^{L,q}(\varepsilon_j))$ denote the total number of degrees of freedom.*

Then there exists a λ_0 (depending on Ω, A, c , and the parameters characterizing the mesh family $\mathcal{T}_{min,\lambda}^{L,q}$) such that for any $\lambda \in (0, \lambda_0]$ there are constants $C, b > 0$ (depending additionally on the implied constants in $q \simeq L \simeq K$) such that

$$\|\mathcal{L}^{-s}f - Q_k^{-s}(\mathcal{L}_{hp})f\|_{\mathbb{H}^s(\Omega)} \leq C \exp(-b\sqrt[5]{N}).$$

6.2.2 Case B

Instead of approximating the problems (6.7) from individual spaces, one may approximate them from the same hp-FE space in Ω . Specifically, we define the approximations w_j^{hp} by: Find $w_j^{hp} \in S_0^q(\Omega, \mathcal{T}_{geo,\sigma}^{L,n})$ such that

$$\forall v \in S_0^q(\Omega, \mathcal{T}_{geo,\sigma}^{L,n}) : a_{\varepsilon_j^2, \Omega}(w_j^{hp}, v) = \langle f, v \rangle. \quad (6.18)$$

Theorem 4 *Let Ω be a curvilinear polygon as defined in Section 1.1 and assume that A, f satisfy (1.1) and that A is uniformly symmetric positive definite. Let u be solution to (1.4), and let its discrete approximation $Q_k^{-s}(\mathcal{L}_{hp})f$ be given by (6.5) in conjunction with (6.18). Fix $c_1 > 0$. Let $K \simeq q \simeq L = n$ and let $N = (2K+1) \dim S_0^q(\Omega, \mathcal{T}_{geo,\sigma}^{L,n}) \sim q^6$ denote the total number of degrees of freedom.*

Then, under the scale resolution condition

$$\sigma^L \leq c_1 e^{-K/2} \quad (6.19)$$

there are constants $C, b > 0$ (depending on $\Omega, A, f, c_1, \sigma$, and the analyticity properties of the macro triangulation) such that

$$\|\mathcal{L}^{-s}f - Q_k^{-s}(\mathcal{L}_{hp})f\|_{\mathbb{H}^s(\Omega)} \leq C \exp(-b\sqrt[6]{N}).$$

Proof The proof follows the arguments of Theorem 3. Since $e^{-K/2} = \min_j \varepsilon_j$ is the smallest scale, the scale resolution condition (6.19) ensures that Proposition 1 is applicable.

7 Numerical experiments

We consider the problem (1.4) with diffusion coefficient $A = I$, i.e., $\mathcal{L}^s = (-\Delta)^s$. The domain Ω is chosen as either the unit square $\Omega_1 = (0, 1)^2$, the so-called L -shaped polygonal domain $\Omega_2 \subset \mathbb{R}^2$ determined by the vertices $\{(0, 0), (1, 0), (1, 1), (-1, 1), (-1, -1), (0, -1)\}$, or the square domain with a slit $\Omega_3 = (-1, 1)^2 \setminus (-1, 0] \times \{0\}$. As we are in particular interested in smooth, but possibly non-compatible data f in all the numerical examples we take

$$f(x_1, x_2) \equiv 1 \quad \text{in } \Omega. \quad (7.1)$$

Notice that, in this case, f is analytic on $\overline{\Omega}$ but $f \in \mathbb{H}^{1-s}(\Omega)$ only for $s > 1/2$ due to boundary incompatibility (cf. Remark 1). The exact solution is not known, so that the error is estimated numerically with reference to an accurate numerical solution. The error measure is always the functional

$$e(\tilde{u}) = \left| d_s \int_{\Omega} f(u^{\text{fine}} - \tilde{u}) \, dx' \right|^{1/2}, \quad (7.2)$$

where u^{fine} is the numerical solution obtained on a fine mesh. Note that for the Galerkin method on the cylinder \mathcal{C} (i.e., Extended hp -FEM in **Case B**) this error measure is equivalent to the energy norm if u^{fine} is replaced by the exact solution u :

$$\|u - \text{tr}_{\Omega} \mathcal{U}^p\|_{\mathbb{H}^s(\Omega)}^2 \lesssim \|\nabla(\mathcal{U} - \mathcal{U}^p)\|_{L^2(y^\alpha, \mathcal{C})}^2 = d_s \int_{\Omega} f(u - \text{tr}_{\Omega} \mathcal{U}^p) \, dx',$$

where \mathcal{U}^p denotes the discrete solution in $\mathcal{C}_{\mathcal{Y}}$.

In Figure 4 we show examples of the meshes used for the three domains. These are constructed using the Netgen/NGSolve package [35]. For the square domain $\Omega = \Omega_1$ the resulting mesh is the geometric boundary layer mesh $\mathcal{T}_{geo, \sigma_x}^{L, L}$ with $L = 4$ and $\sigma_x = 1/4$. The same parameters are used in Netgen/NGSolve to construct the meshes for the other two domains, with the resulting meshes diverging from the strict definition of $\mathcal{T}_{geo, \sigma_2}^{L, L}$ near the re-entrant corners since these meshes are not constructed using mesh patches but instead by applying directly geometric refinement towards edges and vertices. Nevertheless we denote these meshes also by $\mathcal{T}_{geo, \sigma_x}^{L, L}$ and make use of the finite element spaces $S_0^q(\Omega, \mathcal{T}_{geo, \sigma_x}^{L, L})$.

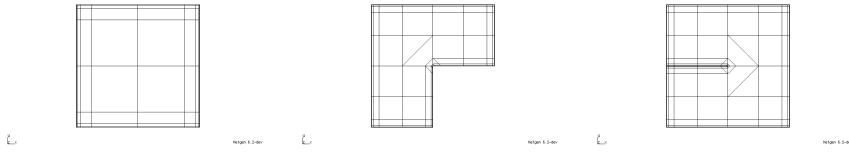


Fig. 4 Examples of geometric boundary layer meshes generated by Netgen/NGSolve [35] that are used for the three domains $\Omega = \Omega_j$, $j = 1, 2, 3$, ordered from left to right.

Given a polynomial order $p \geq 1$, in both approaches the finite element space in Ω is $S_0^q(\Omega, \mathcal{T}_{geo, \sigma_x}^{L, L})$ with uniform polynomial degree $q = p$, number of levels $L = p$ and $\sigma_x = 1/4$. Next, we describe the parameters used in the hp -FEM on $(0, \mathcal{Y})$ and the quadrature in the Balakrishnan formula.

For the extended problem, on the geometric mesh $\mathcal{G}_{geo, \sigma_y}^M$ in $(0, \mathcal{Y})$ as defined in Section 2.1.1 we use FE-spaces $S_{\{\mathcal{Y}\}}^{\mathbf{r}}((0, \mathcal{Y}), \mathcal{G}_{geo, \sigma_y}^M)$. Given a polynomial degree $p \geq 1$, in the definition of these spaces we use $\mathcal{Y} = \frac{1}{2}p$, $\sigma_y = 1/4$ and $M = \text{round}(0.79 p/s)^3$, and a uniform degree vector $\mathbf{r} = (p, \dots, p)$.

For simplicity in the analysis of the sinc quadrature, we used a symmetric approximation (6.3). For the numerical experiments in order to obtain a more efficient scheme we have followed [9] to define the quadrature as

$$Q_k^{-s}(\mathcal{L})f := \frac{k \sin(\pi s)}{\pi} \sum_{\ell=-K_1}^{K_2} e^{-sy_\ell} (I + e^{-y_\ell} \mathcal{L})^{-1} f, \quad (7.3)$$

with $y_\ell = \ell k$ and the number of quadrature points chosen as

$$K_1 = \left\lceil \frac{\pi^2}{2(1-s)k^2} \right\rceil, \quad K_2 = \left\lceil \frac{\pi^2}{sk^2} \right\rceil.$$

For the given polynomial order $p \geq 1$, we set $k = \frac{4}{3}p^{-1}$.

We now compare the convergence of the two schemes. We plot the error against the polynomial degree p and against $N_{\text{ls}}^{1/2}$, where N_{ls} is the number of linear systems that need to be solved. The convergence curves for the square domain Ω_1 are shown in Figure 5, for the L-shaped domain Ω_2 in Figure 6, and for the slit domain Ω_3 in Figure 7. For all three domains we clearly see exponential convergence as the polynomial order is increased. Also, the Extended hp -FEM requires significantly fewer linear systems to be solved to achieve the same accuracy as the sinc BK-FEM. We should, however, also note that the eigenvalue problem (3.2) becomes ill-conditioned for increasing p and much higher accuracy than the one shown in the above figures cannot be obtained using our approach for the extension problem. No such accuracy limitations could be seen for the sinc approach.

8 Extensions and Conclusions

8.1 Fractional Diffusion on Manifolds

We describe next *fractional surface diffusion operators on analytic manifolds*, that are of interest in some application. It exploits the admissibility of non-constant, analytic coefficient $A(x')$ in the diffusion operator \mathcal{L} . The numerical schemes and their analysis as described above can be extended to this setting as well.

³ The choice $M = \text{round}(0.79 p/s)$ resulted from equilibrating (an upper bound) for the semidiscretization error associated with $[y_0, y_1]$ and $[y_{M-1}, y_M]$

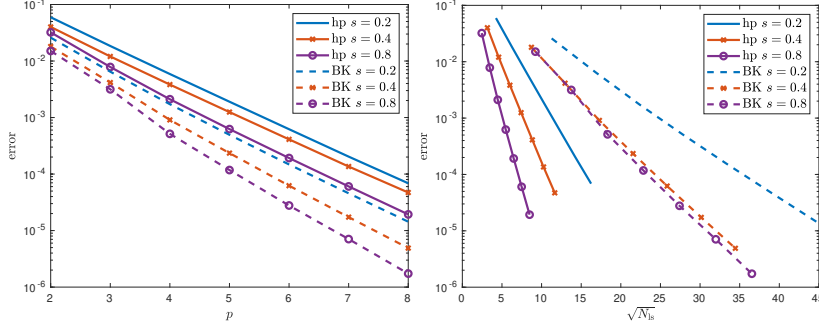


Fig. 5 Error convergence of the Extended hp -FEM and the sinc BK-FEM for the domain Ω_1 , depicted versus the polynomial degree p and $N_{ls}^{1/2}$, where N_{ls} denote the number of linear systems that need to be solved. Solid lines correspond to Extended hp -FEM and dashed lines to the sinc BK-FEM. Results for $s = 0.2$, $s = 0.4$ and $s = 0.8$ are shown.

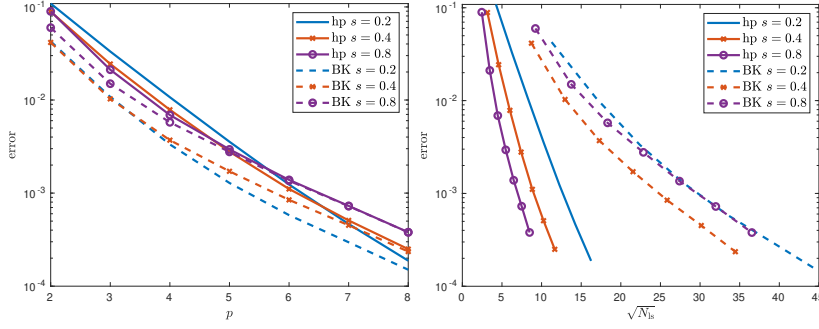


Fig. 6 Error convergence of the Extended hp -FEM and the sinc BK-FEM for L-shaped domain Ω_2 , depicted versus the polynomial degree p and $N_{ls}^{1/2}$, the square root of the number of linear systems to be solved.

Let $\Gamma \subset \mathbb{R}^3$ denote a compact, orientable analytic manifold (e.g. [3]). We think of bounded, analytic surfaces such as the unit sphere $\mathbb{S}^2 \subset \mathbb{R}^3$. Let Γ be covered by a finite atlas of analytic charts $\{\chi_j\}_{j=1}^J$. In a generic analytic chart χ of Γ , consider the polygonal domain $\tilde{\Gamma} = \chi(\Omega) \subset \Gamma$ where the parameter domain $\Omega \subset \mathbb{R}^2$ of the chart χ is a curvilinear polygon in the sense of Section 1.1. On Γ , introduce the surface (Lebesgue)measure μ . On $\tilde{\Gamma}$, for given $\tilde{f} \in L^2(\Gamma, \mu; \mathbb{R})$, consider the *Dirichlet problem for the surface diffusion operator* $\tilde{\mathcal{L}}$: find u_Γ such that

$$\tilde{\mathcal{L}}u_\Gamma := -\operatorname{div}_\Gamma(\tilde{A}\nabla_\Gamma u_\Gamma) = \tilde{f} \quad \text{on} \quad \tilde{\Gamma}, \quad u_\Gamma|_{\partial\tilde{\Gamma}} = 0. \quad (8.1)$$

Here, the “diffusion coefficient” \tilde{A} in (8.1) is a symmetric, uniformly in Γ positive definite linear map acting on the tangent bundle of Γ , and ∇_Γ and $\operatorname{div}_\Gamma$ denote the surface gradient and divergence differential operators on Γ , respectively (see [3]). With Sobolev spaces on Γ invariantly defined in the usual fashion (e.g., [3]), the surface diffusion operator $\tilde{\mathcal{L}}$ in (8.1) extends to

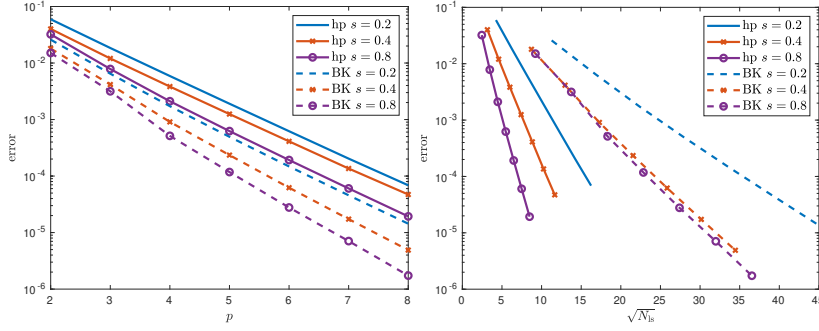


Fig. 7 Error convergence of the Extended hp -FEM and the sinc BK-FEM for the slit domain Ω_3 , depicted versus the polynomial degree p and $N_{\text{ls}}^{1/2}$, the square root of the number of linear systems to be solved.

a boundedly invertible, self-adjoint operator $\tilde{\mathcal{L}} : H_0^1(\tilde{\Gamma}; \mu) \rightarrow H^{-1}(\tilde{\Gamma}; \mu) = (H_0^1(\tilde{\Gamma}; \mu))^*$ (duality with respect to $L^2(\tilde{\Gamma}; \mu) \simeq (L^2(\tilde{\Gamma}; \mu))^*$) whose inverse $\tilde{\mathcal{L}}^{-1}$ is a compact, self-adjoint operator on $L^2(\tilde{\Gamma}; \mu)$. The spectral theorem implies that $\tilde{\mathcal{L}}^{-1}$ admits a countable sequence of eigenpairs $(\tilde{\lambda}_k, \tilde{\varphi}_k)_{k \geq 1}$ whose eigenvectors $\tilde{\varphi}_k$ can be normalized so that they constitute an ONB of $L^2(\tilde{\Gamma}; \mu)$. With the ONB $\{\tilde{\varphi}_k\}_{k \geq 1}$, fractional Sobolev spaces on $\tilde{\Gamma}$ can be defined as in (1.3), i.e. for $0 < s < 1$,

$$\mathbb{H}^s(\tilde{\Gamma}) := \left\{ w = \sum_{k=1}^{\infty} w_k \tilde{\varphi}_k : \|w\|_{\mathbb{H}^s(\tilde{\Gamma})}^2 = \sum_{k=1}^{\infty} \tilde{\lambda}_k^s w_k^2 < \infty \right\}. \quad (8.2)$$

The space $\mathbb{H}^s(\tilde{\Gamma})$ can be characterized by (real) interpolation: There holds $\mathbb{H}^s(\tilde{\Gamma}) = (H_0^1(\tilde{\Gamma}; \mu), L^2(\tilde{\Gamma}; \mu))_{s,2}$ for $0 < s < 1$. As in (1.4), with the family $(\tilde{\lambda}_k, \tilde{\varphi}_k)_{k \geq 1}$ we may define the spectral fractional Laplacian $\tilde{\mathcal{L}}^s = (\mathcal{L}, I)_{s,2}$ by interpolation of linear operators (e.g. [19]). The arguments in [14] extend verbatim the localization (1.5) to the present setting. In particular, the spectral fractional diffusion operator on $\tilde{\Gamma}$ with homogeneous Dirichlet boundary conditions on $\partial\tilde{\mathcal{L}}$ admits a localization on the cylinder $\tilde{\mathcal{C}} = \tilde{\Gamma} \times (0, \infty)$.

Pulling back the problem (8.1) via χ into the (Euclidean) chart domain $\Omega \subset \mathbb{R}^2$, the Dirichlet problem for the fractional power $s \in (0, 1)$ of the surface diffusion (8.1) in $\tilde{\Gamma} = \chi(\Omega)$ reduces to (1.5) where the bilinear form (1.2) and diffusion coefficient A are given by

$$A(x') = G(x')^\top (\tilde{A} \circ \chi)(x') G(x'), \quad x' \in \Omega,$$

with $G(x') = D\chi(x') : \Omega \rightarrow \mathbb{R}^{3 \times 2}$ denoting the (assumed analytic in $\overline{\Omega}$) metric of \mathcal{M} in chart χ . The real-analyticity of compositions, sums and product of real-analytic functions implies that $A(x')$ satisfies (1.1) in Ω , so that the ensuing mathematical results also apply to (1.4) with (8.1).

8.2 N -widths of solution sets

The hp -approximation rate bounds for either the Extended hp -FEM (Theorems 1, 2) and the sinc BK-FEM (Theorems 3, 4) imply exponential bounds on N -widths of solution sets of (1.4) in a curvilinear polygon Ω as defined in Section 1.1, with the data A and f satisfying the conditions in Section 1.2. Such bounds are well-known to determine the rate of convergence of so-called *reduced basis methods* (see [32] and the references there).

We recall that, for a normed linear space X (with norm $\|\cdot\|_X$) and for a compact subset $\mathcal{K} \subset X$, the N -width of \mathcal{K} in X is given by

$$d_N(\mathcal{K}, X) = \inf_{E_N} \sup_{f \in \mathcal{K}} \inf_{g \in E_N} \|f - g\|_X. \quad (8.3)$$

Here, the first infimum is taken over all subspaces E_N of X of dimension $N \in \mathbb{N}$. Subspace sequences $\{E_N\}_{N \geq 1}$ that attain the rates of $d_N(\mathcal{K}, X)$ in (8.3) as $N \rightarrow \infty$ can be realized numerically by (generally non-polynomial) so-called *reduced bases* (see, e.g., [32] and the references there). Here, we fix a set $G \subset \mathbb{C}^2$ containing $\bar{\Omega}$ and choose $\mathcal{A} \subset L^2(\Omega)$ as the set of functions $f : \Omega \rightarrow \mathbb{R}$ that admit a holomorphic extension to G with $\|f\|_{L^\infty(\Omega)} \leq 1$. Then $\mathcal{K} := \mathcal{L}^{-s}\mathcal{A} \subset \mathbb{H}^s(\Omega)$ is a compact subset by the continuity of $\mathcal{L}^{-s} : \mathbb{H}^{-s}(\Omega) \rightarrow \mathbb{H}^s(\Omega)$ and the compact embedding $L^2(\Omega) \subset \mathbb{H}^{-s}(\Omega)$. We choose $X = \mathbb{H}^s(\Omega)$ in (8.3).

Then, from Theorem 4 and the fact that $Q_k^{-s}(\mathcal{L}_{hp})f \in S_0^q(\Omega, \mathcal{T}_{geo,\sigma}^{L,n})$, with the choices of parameters in Theorem 4, $N = \dim(S_0^q(\Omega, \mathcal{T}_{geo,\sigma}^{L,n})) = O(q^4)$, for \mathcal{K} as above and $E_N = S_0^q(\Omega, \mathcal{T}_{geo,\sigma}^{L,n})$ follows the (constructive) bound

$$d_N(\mathcal{K}, X) \lesssim \exp(-b\sqrt[4]{N}) \quad (8.4)$$

for some constant $b > 0$ independent of N .

We also mention that the argument in [26] can be adapted to the setting of (1.4) in Section 1.1, resulting in the (sharp) nonconstructive bound

$$d_N(\mathcal{K}, X) \lesssim \exp(-b\sqrt{N}). \quad (8.5)$$

We refer to [1, 12, 16] for numerical approximation of (1.4) using reduced basis methods.

8.3 Conclusions

For the Dirichlet problem of the spectral, fractional diffusion operator \mathcal{L}^s with $0 < s < 1$ in a bounded, polygonal domain $\Omega \subset \mathbb{R}^2$, we proposed two hp -FE discretizations. The first discretization, already considered in [8, 23], is based on the CS-extension upon hp -FE *semi-discretization in the extended variable*. Subsequent diagonalization leads to a decoupled system (3.5) of \mathcal{M} linear and local, singularly perturbed second order reaction-diffusion problems in Ω . Invoking analytic regularity results for these problems from [27, 29], and *robust*

exponential convergence of hp -FEM for reaction-diffusion problems in polygons from [7, 27, 28], an exponential convergence rate bound $C \exp(-b \sqrt[6]{N_{DOF}})$ with respect to the total number of degrees of freedom, N_{DOF} , which are used in the tensor-product hp -FE discretization, is established in the fractional Sobolev norm $\mathbb{H}^s(\Omega)$. We add that the variational semi-discretization in Section 3 with respect to the extruded variable y offers the possibility for *residual a posteriori* error estimation.

The second discretization is based on the spectral integral representation of \mathcal{L}^{-s} due to Balakrishnan [6]. A sinc quadrature discretization [39] approximates the spectral integral by an (exponentially convergent [10, 39]) finite linear combination of solutions of decoupled elliptic reaction diffusion problems in Ω with analytic input data. Drawing once more on analytic regularity and robust exponential convergence of hp -FEM [7, 27–29], we prove exponential convergence also for this approach. A computable *a posteriori* bound for the semidiscretization error incurred for the sinc BK-FEM approach does not seem to be available currently.

The theoretical convergence rate bounds are verified in a series of numerical experiments. These show, in particular, that exponential convergence is realized in the practical range of discretization parameters. They also indicate a number of practical issues, such as conditioning or algorithmic steering parameter selection, which are beyond the scope of the mathematical convergence analysis. We point out that the proposed algorithms and the exponential convergence results extend in several directions: besides homogeneous Dirichlet boundary conditions, also mixed, Dirichlet-Neumann boundary conditions, and operators with a nonzero first order term could be considered. In either case, the proposed algorithms extend readily. The main result is the construction of hp -FE discretizations with robust exponential convergence rates for spectral fractional diffusion in polygonal domains $\Omega \subset \mathbb{R}^2$. Similar results hold in bounded intervals $\Omega \subset \mathbb{R}^1$ (we refer to [8] for details). In polyhedral $\Omega \subset \mathbb{R}^3$, the present line of analysis is also applicable; however, exponential convergence and analytic regularity of hp -FEM for reaction-diffusion problems in space dimension $d = 3$ does not appear to be available to date. We considered fractional powers only for self-adjoint, second-order elliptic divergence-form differential operators $\mathcal{L}w = -\operatorname{div}(A\nabla w)$ in Ω . The arguments for the sinc BK-FEM extend to non-selfadjoint operators which include first-order terms via [9], provided suitable hp -FEM for advection-reaction-diffusion problems in Ω are available (e.g. [24]).

The present analysis is indicative for achieving high, algebraic rate $p+1-s$ of convergence in $\mathbb{H}^s(\Omega)$ by h -version FEM of fixed order $p \geq 1$ in Ω . As in hp -FEM, this will require anisotropic mesh refinement aligned with $\partial\Omega$, ie., so-called “boundary-layer” meshes. Several constructions are available (see, e.g., [38] for so-called “exponential boundary layer meshes” and [33] for so-called “Shiskin meshes”). We refrain from developing details for this approach which can be analyzed along the lines of the present paper.

References

1. Harbir Antil, Yanlai Chen, and Akil Narayan. Reduced basis methods for fractional Laplace equations via extension. *SIAM J. Sci. Comput.*, 41(6):A3552–A3575, 2019.
2. T. Apel and J.M. Melenk. Interpolation and quasi-interpolation in h - and hp -version finite element spaces. In E. Stein, R. de Borst, and T.J.R. Hughes, editors, *Encyclopedia of Computational Mechanics*, pages 1–33. John Wiley & Sons, Chichester, UK, second edition, 2018. extended preprint at <http://www.asc.tuwien.ac.at/preprint/2015/asc39x2015.pdf>.
3. Thierry Aubin. *Some nonlinear problems in Riemannian geometry*. Springer Monographs in Mathematics. Springer-Verlag, Berlin, 1998.
4. I. Babuška and B.Q. Guo. The $h - p$ version of the finite element method. Part 1: The basic approximation results. *Computational Mechanics*, 1:21–41, 1986.
5. I. Babuška and B.Q. Guo. The $h - p$ version of the finite element method. Part 2: General results and applications. *Computational Mechanics*, 1:203–220, 1986.
6. A. V. Balakrishnan. Fractional powers of closed operators and the semigroups generated by them. *Pacific J. Math.*, 10:419–437, 1960.
7. L. Banjai, J.M. Melenk, and Ch. Schwab. hp -FEM for reaction-diffusion equations. II: Robust exponential convergence for multiple length scales in corner domains. Technical Report 2020-28, Seminar for Applied Mathematics, ETH Zürich, Switzerland, 2020.
8. Lehel Banjai, Jens M. Melenk, Ricardo H. Nochetto, Enrique Otárola, Abner J. Salgado, and Christoph Schwab. Tensor FEM for spectral fractional diffusion. *Found. Comput. Math.*, 19(4):901–962, 2019.
9. A. Bonito, W. Lei, and J. E. Pasciak. On sinc quadrature approximations of fractional powers of regularly accretive operators. *J. Num. Math.*, 27(2):57–68, 2019.
10. A. Bonito and J.E. Pasciak. Numerical approximation of fractional powers of elliptic operators. *Math. Comp.*, 84(295):2083–2110, 2015.
11. Andrea Bonito, Juan Pablo Borthagaray, Ricardo H. Nochetto, Enrique Otárola, and Abner J. Salgado. Numerical methods for fractional diffusion. *Comput. Vis. Sci.*, 19(5-6):19–46, 2018.
12. Andrea Bonito, Diane Guignard, and Ashley R. Zhang. Reduced basis approximations of the solutions to spectral fractional diffusion problems, 2020. arXiv:1905.01754.
13. X. Cabré and J. Tan. Positive solutions of nonlinear problems involving the square root of the Laplacian. *Adv. Math.*, 224(5):2052–2093, 2010.
14. L. Caffarelli and L. Silvestre. An extension problem related to the fractional Laplacian. *Comm. Part. Diff. Eqs.*, 32(7-9):1245–1260, 2007.
15. L.A. Caffarelli and P.R. Stinga. Fractional elliptic equations, Caccioppoli estimates and regularity. *Ann. Inst. H. Poincaré Anal. Non Linéaire*, 33(3):767–807, 2016.
16. Tobias Danczul and Joachim Schöberl. A reduced basis method for fractional diffusion operators II, 2020. arXiv:2005.03574.
17. M. Faustmann and J.M. Melenk. Robust exponential convergence of hp -FEM in balanced norms for singularly perturbed reaction-diffusion problems: corner domains. *Comput. Math. Appl.*, 74(7):1576–1589, 2017.
18. Michael Karkulik and Jens Markus Melenk. \mathcal{H} -matrix approximability of inverses of discretizations of the fractional Laplacian. *Adv. Comput. Math.*, 45(5-6):2893–2919, 2019.
19. S. G. Kreĭn. Interpolation of linear operators, and properties of the solutions of elliptic equations. In *Elliptische Differentialgleichungen, Band II*, pages 155–166. Schriftenreihe Inst. Math. Deutsch. Akad. Wissensch. Berlin, Reihe A, Heft 8. Akademie-Verlag, Berlin, 1971.
20. A. Lischke, G. Pang, M. Gulian, F. Song, C. Glusa, X. Zheng, Z. Mao, W. Cai, M. M. Meerschaert, M. Ainsworth, and G. E. Karniadakis. What is the fractional Laplacian? A comparative review with new results. *J. Comput. Phys.*, 404:109009, 62, 2020.
21. Robert E. Lynch, John R. Rice, and Donald H. Thomas. Direct solution of partial difference equations by tensor product methods. *Numer. Math.*, 6:185–199, 1964.
22. W. McLean. *Strongly elliptic systems and boundary integral equations*. Cambridge University Press, Cambridge, 2000.

23. Dominik Meidner, Johannes Pfefferer, Klemens Schürholz, and Boris Vexler. *hp*-finite elements for fractional diffusion. *SIAM J. Numer. Anal.*, 56(4):2345–2374, 2018.
24. Jens Melenk and Christoph Schwab. An *hp* finite element method for convection-diffusion problems in one dimension. *IMA Journal of Numerical Analysis*, 19(3):425–453, 1999.
25. J.M. Melenk. On the robust exponential convergence of *hp* finite element method for problems with boundary layers. *IMA J. Numer. Anal.*, 17(4):577–601, 1997.
26. J.M. Melenk. On *n*-widths for elliptic problems. *J. Math. Anal. Appl.*, 247(1):272–289, 2000.
27. J.M. Melenk. *hp*-finite element methods for singular perturbations, volume 1796 of *Lecture Notes in Mathematics*. Springer-Verlag, Berlin, 2002.
28. J.M. Melenk and Ch. Schwab. *hp* FEM for reaction-diffusion equations. I. Robust exponential convergence. *SIAM J. Numer. Anal.*, 35(4):1520–1557, 1998.
29. J.M. Melenk and Ch. Schwab. Analytic regularity for a singularly perturbed problem. *SIAM J. Math. Anal.*, 30(2):379–400, 1999.
30. J.M. Melenk and C. Xenophontos. Robust exponential convergence of *hp*-FEM in balanced norms for singularly perturbed reaction-diffusion equations. *Calcolo*, 53(1):105–132, 2016.
31. R.H. Nochetto, E. Otárola, and A.J. Salgado. A PDE approach to fractional diffusion in general domains: a priori error analysis. *Found. Comput. Math.*, 15(3):733–791, 2015.
32. Alfio Quarteroni, Andrea Manzoni, and Federico Negri. *Reduced basis methods for partial differential equations*, volume 92 of *Univtext*. Springer, Cham, 2016. An introduction, La Matematica per il 3+2.
33. Hans-Görg Roos, Martin Stynes, and Lutz Tobiska. *Robust numerical methods for singularly perturbed differential equations*, volume 24 of *Springer Series in Computational Mathematics*. Springer-Verlag, Berlin, second edition, 2008. Convection-diffusion-reaction and flow problems.
34. Xavier Ros-Oton. Nonlocal elliptic equations in bounded domains: a survey. *Publ. Mat.*, 60(1):3–26, 2016.
35. J. Schöberl. Netgen an advancing front 2d/3d-mesh generator based on abstract rules. *J. Comput. Visual. Sci.*, 1:41–52, 1997.
36. Ch. Schwab. *p- and hp-Finite Element Methods*. Numerical Mathematics and Scientific Computation. The Clarendon Press, Oxford University Press, New York, 1998. Theory and applications in solid and fluid mechanics.
37. Ch. Schwab and M. Suri. The *p* and *hp* versions of the finite element method for problems with boundary layers. *Math. Comp.*, 65(216):1403–1429, 1996.
38. Ch. Schwab, M. Suri, and C.A. Xenophontos. The *hp* Finite Element Method for problems in mechanics with boundary layers. *Comp. Meth. Appl. Mech. Engg.*, 157(3-4):311–333, 1998.
39. Frank Stenger. *Numerical methods based on sinc and analytic functions*, volume 20 of *Springer Series in Computational Mathematics*. Springer-Verlag, New York, 1993.
40. P.R. Stinga and J.L. Torrea. Extension problem and Harnack’s inequality for some fractional operators. *Comm. Partial Differential Equations*, 35(11):2092–2122, 2010.